JANUARY 2022

M.Sc. in Civil Engineering

YASHAR ALI

REPUBLIC OF TURKEY

GAZİANTEP UNIVERSITY

GRADUATE SCHOOL OF NATURAL & APPLIED SCIENCES

FLEXURAL BEHAVIOR OF CONCRETE-FILLED STEEL TUBE COMPOSITE BEAMS WITH DIFFERENT ASPECT RATIO

M.Sc. THESIS

IN

CIVIL ENGINEERING

BY

YASHAR ALI

JANUARY 2022

FLEXURAL BEHAVIOR OF CONCRETE-FILLED STEEL TUBE COMPOSITE BEAMS WITH DIFFERENT ASPECT RATIO

M.Sc. Thesis

in

Civil Engineering

Gaziantep University

Supervisor

Assoc. Prof. Dr. Nildem TAYŞİ

Co-Supervisor

Dr. Farid H. ARNAO'T

by

Yashar ALI

January 2022

I hereby declare that all information in this document has been obtained and presented in accordance with academic rules and ethical conduct. I also declare that, as required by these rules and conduct, I have fully cited and referenced all material and results that are not original to this work.

Yashar ALI

ABSTRACT

FLEXURAL BEHAVIOR OF CONCRETE-FILLED STEEL TUBE COMPOSITE BEAMS WITH DIFFERENT ASPECT RATIO

ALI, Yashar
M.Sc. in Civil Engineering
Supervisor: Assoc. Prof. Dr. Nildem TAYŞİ
Co-Supervisor: Dr. Farid H. ARNAO'T
January 2022
57 pages

The objective of the current work is to study the flexural behavior of Concrete-Filled Steel Tube (CFST) composite beams with different aspect ratios. The composite CFST consists of a steel tube filled with Lightweight Concrete (LWC) and a doubly reinforced deck slab of normal concrete. The perfobond shear connector connects the CFST beam and deck slab. Six CFST composite beams were tested; five were filled with LWC, while the sixth hollow beam was used as a control specimen. The main investigated parameters were the effect of the beam aspect ratio (width/depth) and the slab thickness. Three used aspect ratios were (0.4, 0.5, and 0.6). These specimens were compared with the control beam, and three more slabs of variable thickness (75, 85, 100 mm) were used to investigate the effect of slab thickness on the behavior of composite beam. The slabs were doubly reinforced with conventional reinforcement of 6 mm diameter in each direction for all the specimens. Additionally, to investigate the effect of the connector, push out tests are done on three specimens. All specimens were supported and tested using one-point loading. The deflections at midspans and slips produced from the monotonically increased loads were recorded. The results showed that the filled LWC was significantly improved the flexural behavior of the composite beams. On the other hand, the slab with relatively high thickness shows less improvement in composite beam ductility, and this is not surprisingly based on the size effect.

Keywords: Steel Filled Tube, Composite Beam, Perfobond Connector, Slips.

ÖZET

FARKLI GÖRÜNTÜ ORANINDA BETON DOLGU ÇELİK BORU KOMPOZİT KİRİŞLERİN EĞİLME DAVRANIŞI

ALI, Yasher
Yüksek Lisans Tezi, İnşaat Mühendisliği
Danışman: Doç. Dr. Nildem TAYŞİ
Yardımcı Danışman: Dr. Farid H. ARNAO'T
Ocak 2022
57 sayfa

Mevcut çalışmanın amacı, farklı en boy oranlarına sahip Beton Dolgulu Çelik Boru (CFST) kompozit kirişlerin eğilme davranışını incelemektir. Kompozit CFST, Hafif Beton (LWC) ile doldurulmuş bir çelik borudan ve iki kat güçlendirilmiş normal beton güverte levhasından oluşur. Perfobond kesme konektörü, CFST kirişini ve güverte levhasını birbirine bağlar. Altı CFST kompozit kiriş test edildi; beşi LWC ile doldurulmuş, altıncı içi boş kiriş ise kontrol numunesi olarak kullanılmıştır. Araştırılan ana parametreler, kiriş en-boy oranı (genişlik/derinlik) ve döşeme kalınlığının etkisiydi. Kullanılan üç en boy oranı (0.4, 0.5 ve 0.6) idi. Bu numuneler kontrol kirişi ile karşılaştırıldı ve döşeme kalınlığının kompozit kiriş davranışı üzerindeki etkisini araştırmak için değişken kalınlıkta (75, 85, 100 mm) üç döşeme daha kullanıldı. Tüm numuneler için plakalar her yönde 6 mm çapında geleneksel donatı ile iki kat güçlendirilmiştir. Ek olarak, konektörün etkisini araştırmak için üç numune üzerinde dışarı itme testleri yapılır. Tüm numuneler, tek nokta yükleme kullanılarak desteklenmiş ve test edilmiştir. Orta açıklıklardaki sehimler ve monoton artan yüklerden kaynaklanan kaymalar kaydedildi. Sonuçlar, doldurulmuş LWC'nin kompozit kirişlerin eğilme davranışını önemli ölçüde iyileştirdiğini gösterdi. Öte yandan, nispeten yüksek kalınlığa sahip döşeme, kompozit kiriş sünekliğinde daha az gelişme gösterir ve bu, boyut etkisine bağlı olarak şaşırtıcı değildir.

Anahtar Kelimeler: Çelik Dolgulu Boru, Kompozit Kiriş, Perfobond Bağlayıcı ve Slipler

"Dedicated to my family"

ACKNOWLEDGEMENTS

First praise is to Allah, the Almighty, on whom ultimately, we depend for sustenance and guidance. I am ever grateful to ALLAH, the Creator and the Guardian, and to whom I owe my very existence.

Then, I would like to express my special appreciation and thanks to my supervisor, Assoc. Prof. Dr. Nildem TAYŞİ, for all her help, patience, valuable advice, always providing and guiding me in the right direction. I'm very grateful and proud to work under her academic guidance. I would like to express truthful appreciation to my co-supervisor, Dr. Farid H. ARNA'OT, for his guidance, and support throughout this study.

Special thanks to my family for their support and encouragement for me during the years of my study. I am also very thankful to my friends Mustafa TAIFOR & Mustafa F. HASAN for their guidance, advice, and help in preparing and arranging the thesis chapters.

I want to thank everyone who has contributed from far and close to the realization of this study.

LIST OF CONTENT

Page

LIST OF TABLES

Page

LIST OF FIGURES

Page

LIST OF SYMBOLS

F'_c	Concrete Cube Compressive Strength
f'_c	Strength of concrete
f_y	Yield strength of steel
f_u	The ultimate strength of steel
f_{ct}	Ultimate tensile strength of concrete
P	Applied force
L	Length of the specimen
W_t	Width of steel tube
W_s	Width of deck slab
H	Height
δ_u	Centric slip
P_u	Ultimate resistance
Q	Shear capacity
A_c	Shear area
A_{sx}	Area of the transverse rebars
d_{rib}	Diameter of the rib hole
h_{rib}	Height of the rib
t_{rib}	The thickness of the rib
d_b	Bar Diameter
L_c	Contact length between the concrete slab and the steel beam flange
ρ_{long}	Longitudinal reinforcement ratio
ρ_{trans}	Transverse reinforcement ratio

LIST OF ABBREVIATIONS

SP	Superplasticizer
NAS	Normal Aggregate Size
NWC	Normal Weight Concrete
LWC	Lightweight Concrete
LWAC	Lightweight Aggregate Concrete
SLWC	Structural Lightweight Aggregate Concrete
CFST	Concrete Filled Steel Tube
ACI	American Concrete Institute
STCB	Steel Tube Composite Beams
ASTM	American Society For Testing And Materials
NSC	Normal Strength Concrete
AASHTO	American Association of State Highway and Transportation Officials

CHAPTER I

INTRODUCTION

1.1 General

The composite beam utilizes the material properties of both steel and concrete. It is more ductile, has higher strength, and is cheaper than its equivalent steel sections [1–4]. The concrete and steel act together as a composite in the construction and enhance its ultimate capacity and stiffness. Moreover, filling the tube with concrete will decrease the expected local buckling of the steel tube and improve the ultimate resisting load [5, 6]. Recently, the use of Concrete Filled Steel Tube (CFST) members has become common in buildings, bridges, and other structures [7, 8]. The CFST members are used in the moment-resisting frames that need for putting stiff elements in panel zones and zones of demanded high strain [9]. The use of CFST members in moment resisting frames decreases the need for combining rigid elements in panel zones and zones that require high strain. Bridges with CFST members are projected to reduce noise and vibration levels related to pure steel members [10]. Also, the CFST members have been proven to be cost-effective in building structures [11–13]. Some applications of the CFST members are shown in Figure 1.1. The CFST members behave better than hollow tubes [14]. This improvement will be enhanced if the filled concrete has confined [15]. Although there are wide applications of this type of structural member, a few research can be found in the literature.

1.2 Steel Tube Composite Beams (STCB)

When combining two or more types of structural sections, a new member is formed, the produced structural member is known as the composite member. But the original members must be installed appropriately to take advantage of the properties of these materials to resist external loads. For example, in the composite beam and slab, the

shear connector is used to connect them. Figure 1.2 shows the details of the composite beam. Moreover, Figure 1.3 shows the applications of the STCB.

Figure 1.1 Some applications of the CFST members

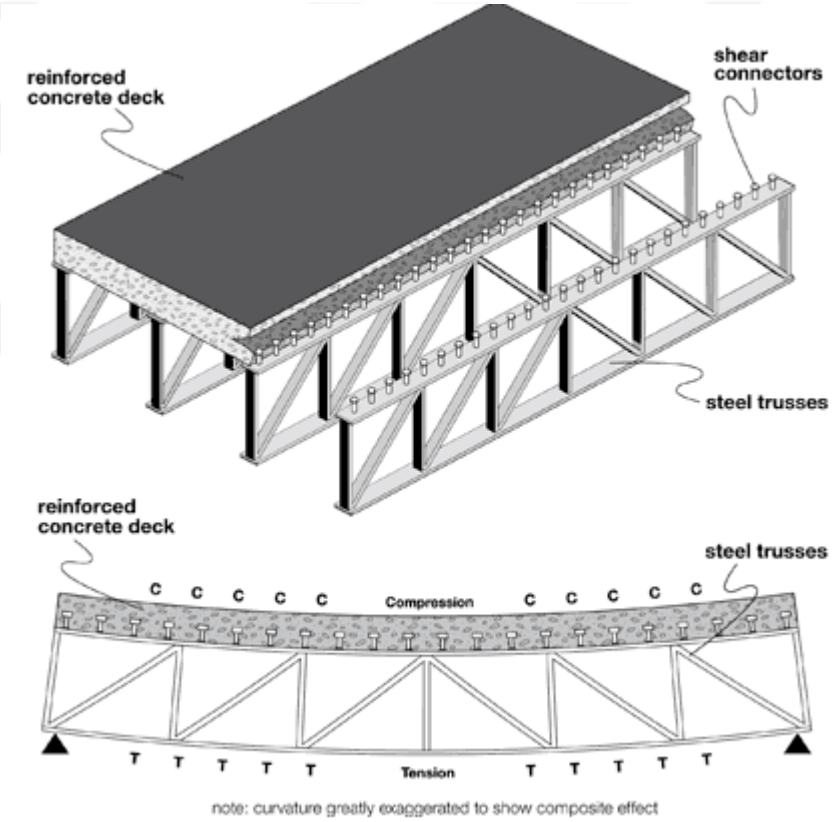

Figure 1.2 Details of the composite beam

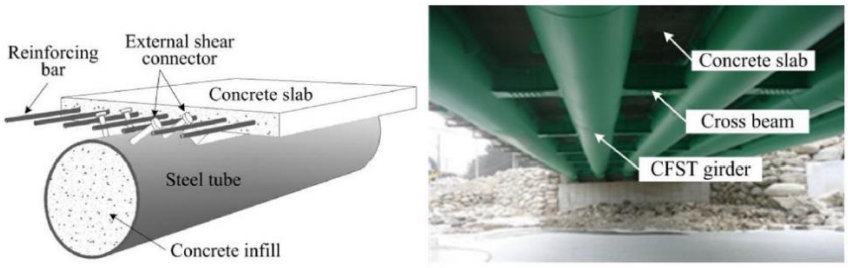

Figure 1.3 Applications of the STCB

1.3 Shear Connectors

In a composite structure, the connection between the structural members plays an important role. For example, the shear connector provides the required shear for composite action in flexure in slab-beam connection. It distributes the large horizontal mechanical phenomenon forces within the block (deck slab) to the chief lateral load resisting structure components. Throughout the earthquake, shear connectors were subjected to cyclic loading [19]. This element of a composite member guarantees the shear transmission between the steel section and the concrete deck slab [20]. Therefore, connecting the concrete deck slab and steel girders could be, in all probability, economic. Figure 1.4 shows a composite beam with a shear stud connection. There are many types of shear connections; headed stud, channel connectors, waveform strip, perfobond ribs, and oscillating perfobond ribs. These types are shown in Figure 1.5.

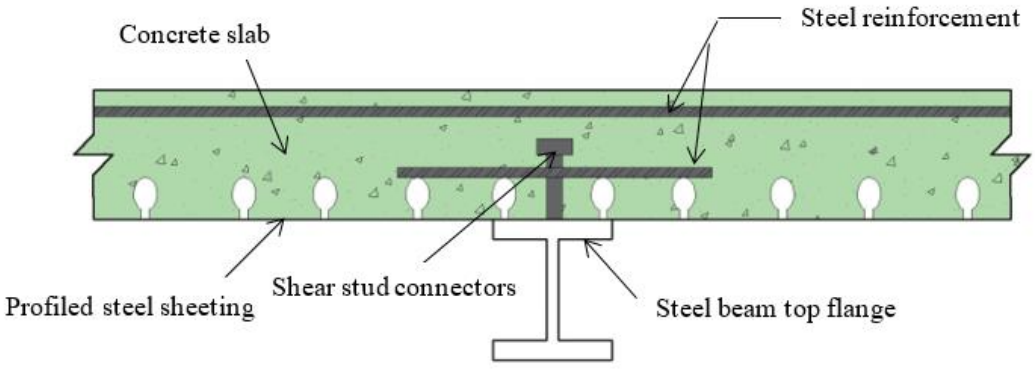

Figure 1.4 Composite beam with shear stud connector

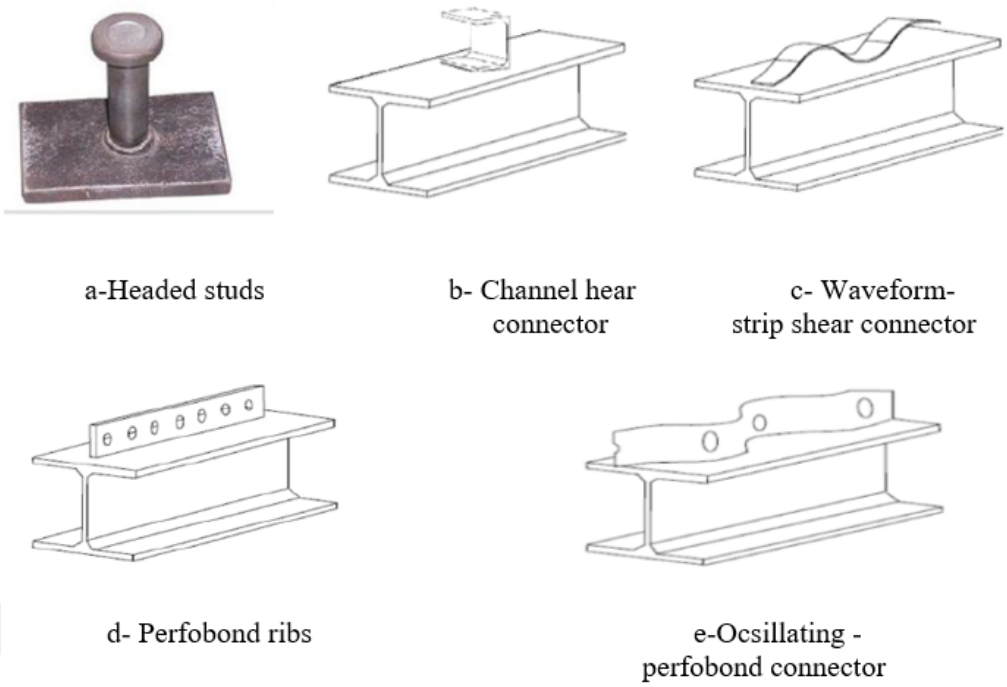

Figure 1.5 Type of shear connector

1.4 Concrete Filled Steel Tubes

CFST members consist of a steel tube filled with concrete material. The infill concrete prevented the steel tube from local buckling inward. Meanwhile, the steel tube confines the concrete. The resulting stress is triaxial compression stress of the concrete and thus can increase the strength, stiffness, load-carrying ability, and flexibility of the structure. The CFST members have numerous advantages compared with any other construction members. In the case of using the column as CFST, this will increase the space used on the floor. The concrete creep and shrinkage of CFST members are much smaller than in ordinary reinforced concrete. It provides excellent seismic resistance. It also exhibits good hysteresis under cyclic loading. The steel tube works as a formwork to pour concrete, leading to a cleaner construction site and saving manpower and project cost and time. Lightweight Concrete (LWC) is used to fill the steel tube to make a lightweight combination of CFST to decrease the self-weight of CFST members [21]. Figure 1.6 shows the typical cross-sections of CFST members. One of the major deterrents to the extensive use of CFST members is little knowledge concerning their performance. Many factors complicate CFST members' design, and analysis are complicated, where the CFST section consists of two items with clearly

different performance and different stress-strain curves. The interaction between core concrete and steel tube is hard in calculating mutual characteristics such as the second moment and elastic modulus. The filling mechanism relies mainly on the steel tube shape and dimensions and the strengths of concrete and steel. Parameters such as concrete sequestration, bond, residual stresses, and loading type also affect the performance of CFST members.

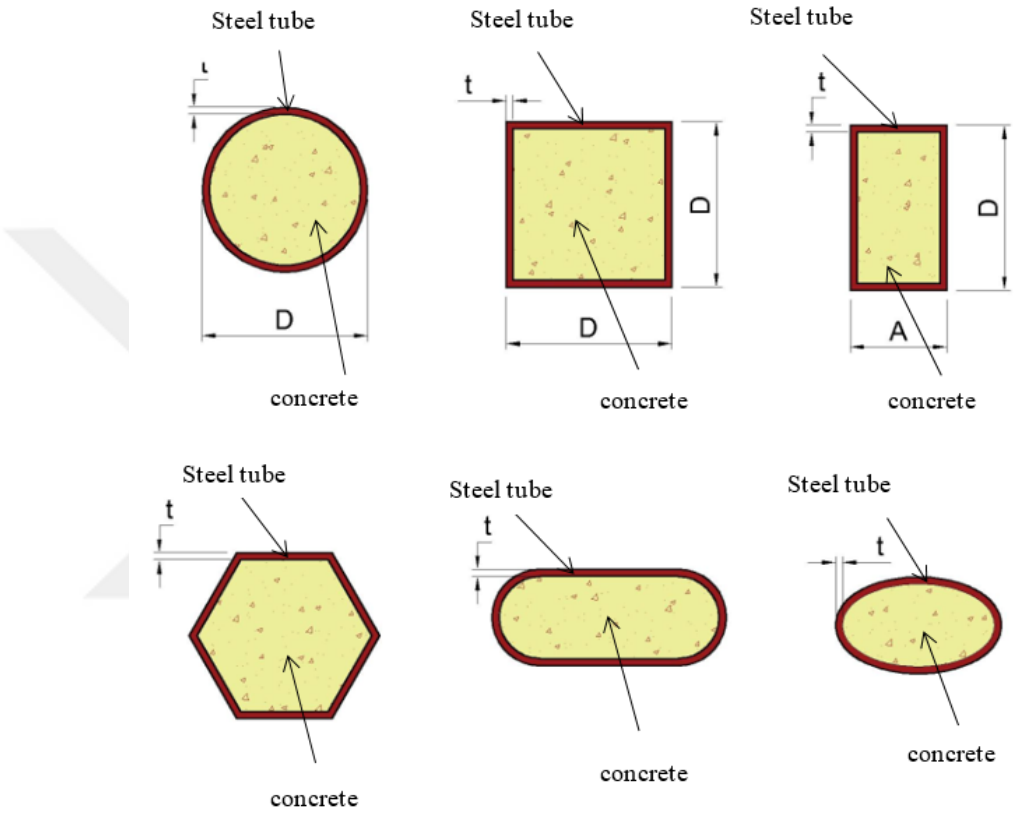

Figure 1.6 Typical sections of concrete filled steel tube

1.5 Objectives of The Study

The main objective of the current study is to test the composite of CFST with the concrete deck slab connected by a perfobond connector. This general goal is divided into the following objectives:

1. Investigate the performance of the end slip and the deflection of composite CFST beam with deck slab experimentally. Therefore, six composite beams are tested under a concentrated load until it fails.

2. Experimental investigation of the performance of perfobond connection by using the push out test; three specimens are tested for this purpose.

1.6 Thesis Layouts

A concise summary of each chapter contained in this thesis is as follow:

Chapter One gives a general introduction about composite members, shear connectors, advantages CFST, objectives, and Scope of the work.

Chapter Two reviews previous investigations about the composite CFST beam with the deck slab.

Chapter Three describes the experimental work, characteristics of steel and concrete, specimen numbers, and types.

Chapter Four presents the experimental work results and discussion.

Chapter Five presents several conclusions and recommendations for the study.

CHAPTER II

LITERATURE REVIEW

2.1 General

(The main aim of this chapter is to provide a review of the essential research found in the literature. The first use of CFST members in China as columns in the large buildings in the early 1950s [22], the CFST columns were used to reduce the size of columns because of their ability to carry heavy load [23]. The first experimental testing of CFST columns was performed in 1957 [24]. The rectangular or circular CFST members are investigated under various load conditions such as axial compression, bending, shear, and twisting [25–30]. These investigations have demonstrated that circular CFST columns offer the best confinement to the filled concrete in steel tubes. In contrast, rectangular CFST is still commonly used in construction for many reasons, including simple basic beam design, simple construction, high flexural stiffness of the section, and esthetic requirements. It also expressed that the strength and rigidity of the CFST members depend on several parameters, e.g., (i) compressive strength of infill concrete, (ii) steel tube yield strength, (iii) steel tube wall thickness, etc.

The use of CFST composite girder as a bridge girder is considered a modern method; Nakamura et al. [10] proposed this system in 2002 for the first time. This system of composite bridge structure offers many benefits; the steel tube acts as a formwork; the concrete avoids the local buckling of the steel tube while the steel tube is confining the concrete in the core of the steel tube.

The cost of the CFST composite bridge system is acceptable and less when compared to other types of bridges. However, despite its many advantages, its use is minimal because of its lack of enough studies and tested design procedures of a bridge system [18]. Chinas' designers pioneer this system and have several bridges in which concrete-filled steel tubes technology has been utilized.

2.2 Flexural Behavior of CFST Beam

Han et al. [31] study the flexural behavior of CFST. This study aims to find the flexural capacity of the CFST beam and compare it with several international codes. Many experimental works have been performed, including sixteen specimens, to accomplish these goals. The cross-section of the examined specimens was square. The changes for these experiments are the aspect ratio from 1 to 2, the depth plate thickness ratio varied from 20 to 50, and the concrete compressive strength that filled the tube. All the specimens had an overall length of 1000 mm and were tested under two points load. Han and his co-authors concluded that the hollow steel tube is less ductile than the CFST.

Furthermore, they found that the approach introduced in their study and EC4 is the best way to estimate the ultimate moment. In contrast, AIJ and LRFDAISC are far from the experimental values of the ultimate moment. Based on the results of Han's work, an experimental study involves a collection of tests of 36 rectangular and circular specimens.

Han et al. [32] proposed the CFST beam's ultimate moment and stiffness. The concrete used in their study to infill the steel tube is self-compacted concrete. The parameter of their research includes a cross-sectional type, steel tube material properties, the compressive strength of the Self-Consolidating Concrete filled the steel tube, and a shear span ratio. The specimens were tested with a load of one and two points. The authors found that the CFST beam filled with SCC has similar to that of the CFST beam filled with Normal Concrete (NWC). Furthermore, the shear-span ratio has little effect on the CFST beam behavior. Moreover, they found the equations suggested by Han [31] are good matching ultimate moment.

Lu et al. [33] provided a theoretical study based on the finite element method to study the CFST beam. The concrete damaged plasticity was used to represent the concrete specifications in this analysis. Two types of stress were used to describe the interface between the steel tube and concrete. The first is normal resistance, while the second is tangential resistance. The element S4R represents the steel tube, and the element C3D8R is used to describe concrete. The authors used the specimens tested by Han et al. [32] to verify the FE results of the CFST beam. They got a good agreement between experimental and theoretical results. The results included the ultimate load, the load-

displacement curve, and the failure mode. The strut-tie model can be used to represent the circular CFST beam. The principal inference used is the model of a strut-tie.

Flor et al. [34] studied the construction and performance of CFST within two phases. The first phase deals with concrete filling the steel tube during concrete pouring. The second phase is about the test and analysis of the CFST beam under flexure. The authors studied the defects produced from pouring concrete in the steel tube, two specimens used with a 12 m, the cross-section steel tube dimensions are 250 * 150 mm with 6.3 mm thick. The authors linked two angles on the top and bottom of the specimen. These angles were repeated in each meter, as shown in Figure 2.1 (a). Both ends of the specimen closed by welding a plate of steel. At the top of the steel tube, two holes with a diameter of 100 mm opened at the end of the specimen. These holes have been used to cast the concrete, as seen in Figures 2.1 (b) and (c). The concrete type used in this study was self-compacting concrete. The concrete was cast in the first specimen under pressure, while the second was without pressure. Eight months both specimens left and opened. Many cavities on the top of the steel tube have been observed in a specimen with pressure and without pressure, these cavities vary in size, and their holes averaged 2.99 mm and 1.97 mm. The second part of the study experimented with six specimens for six meters with the same sectional characteristics as in the first part of the experiments. Four specimens were filled with concrete CFST, and the two remaining specimens were hollow. The second part aims to find the effect of CFST and estimate the flexural capacity of the CFST beam based on plastic theory. The result shows that the moment of the CFST beam is 15 % higher than the hollow beam. Also, they found that the ductility of the CFST is better than the ductility of the hollow specimen.

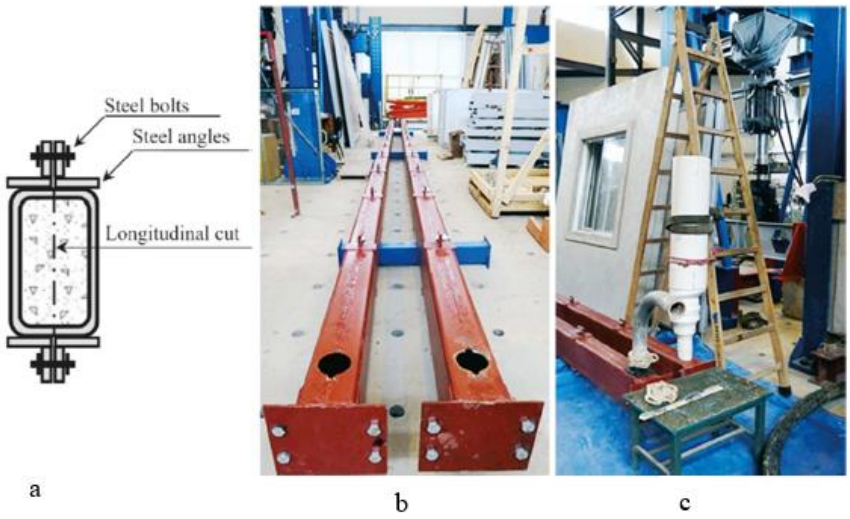

Figure 2.1 CFST specimen details

2.3 Concrete Filled Steel Tube Composite Beam

Hosaka et al. [35] studied the CFST beam; his study consists of two groups. The first group consists of six specimens, and the second group consists of three samples. Specimen M1 was a hollow steel tube, specimens M2, M3, and M4 cast with air mortar. The LWC concrete cast the other specimens (M5 and M6). Specimens of the second group were T1, T2, and T3. Specimen T1 was double skin. The concrete fills the space between two pipes in this specimen. Specimen T2 is identical to that of specimen T1, but specimen T2 is composite with the concrete slab, the steel tube of last specimen T3 is a hollow steel tube composite with a concrete slab. The results show that the steel tube filled with concrete has high moment capacity and more ductility. The ductility had improved if the compressive strength of filling air mortar was more than 5.0 MPa.

This study estimated the cost and construction time of a railway bridge with a length of one kilometer. The study concluded that this type of bridge is feasible and more economical when compared with other types. This study also included that the vibrations and noise in this type of bridge were better when compared with steel bridges.

Nakamura et al. [10] compared multiple bridge styles in Japan. The first type of bridge was a composite girder of concrete-filled steel tubes as a Shinkansen Bridge completed in 2000. The second form was a hybrid of concrete box girder suspended (cable-stay system) and steel girder in the internal part (like Kiso River Bridge). The last type was

a composite steel-concrete girder. The first and second types of bridges are shown in Figure 2.2. The key findings of his study were that the concrete-filled steel tube girder improves the flexural capacity of the bridge because the concrete avoids the local buckling of the steel tube. In addition, the CFST composite bridge improved the performance of the bridge in vibration and noise compared with other types of bridges. Therefore, the study concludes that the extra weight is not a drawback in CFST but was helpful to improve the vibration and noise and prevent the lifting at the first and last support. Furthermore, the equilibrium of cable-stayed bridges was also enhanced. Therefore the authors suggest new bridges (cable stays with CFST girders) as shown in Figure 2.3.

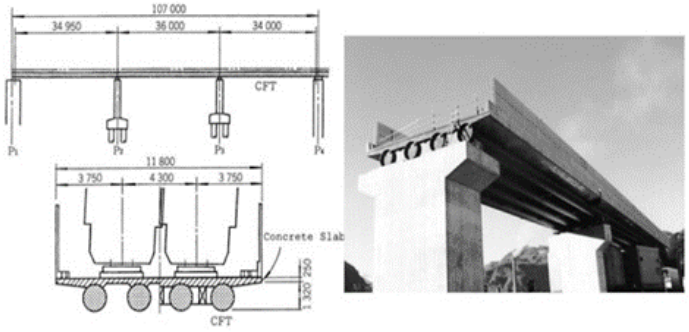

(a) CFST composite bridge (Shinkansen bridge)

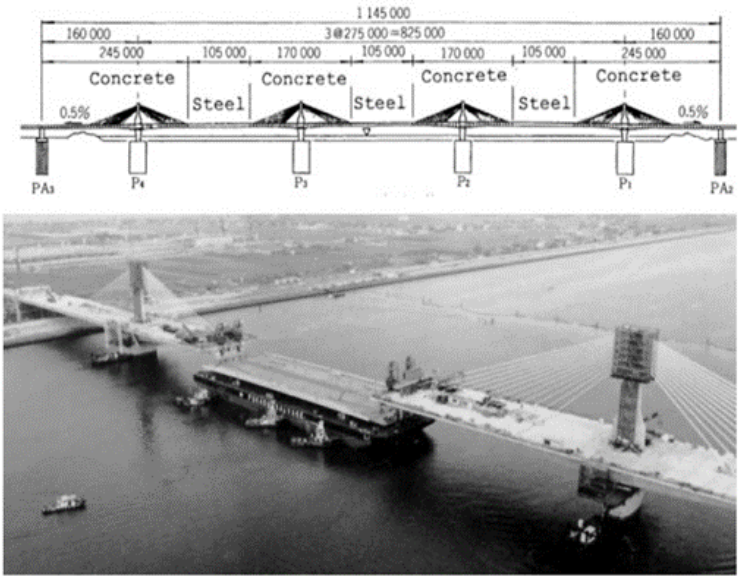

(a) (b) Bridge of Kiso river

Figure 2.2 Type of bridges

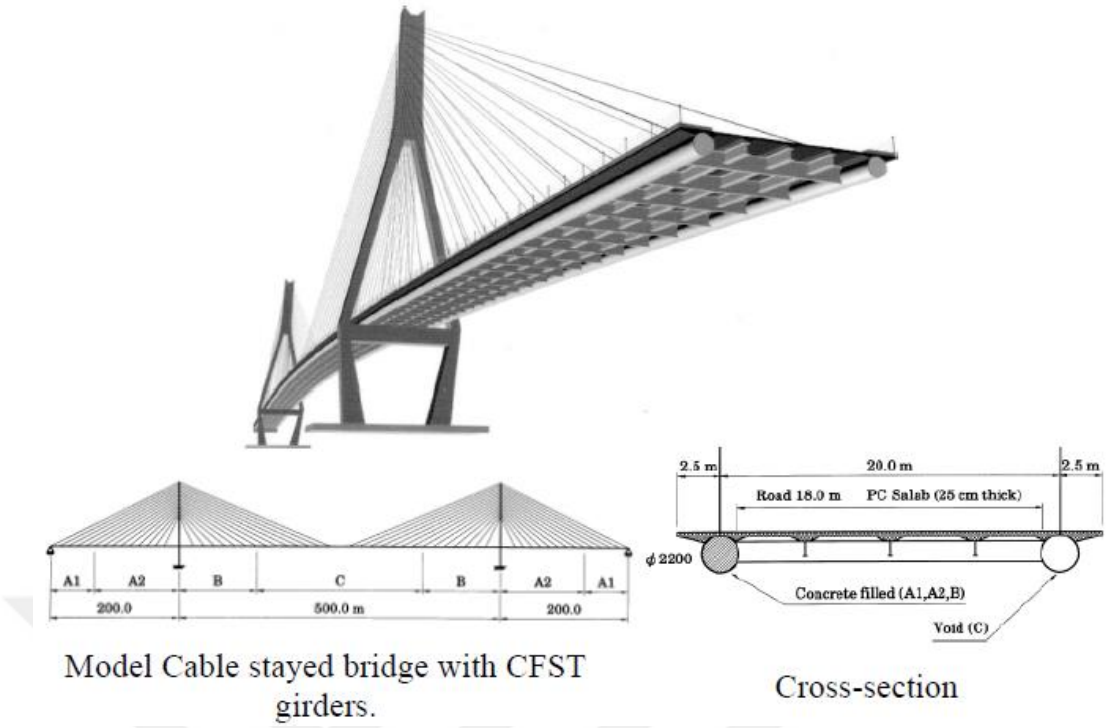

Figure 2.3 Suggested type of bridge by Nakamura et al.

Mossahebi et al. [36] considered that the concrete filled steel composite girders are suitable for constructing bridges. However, the authors considered that the design of this type of bridge faces an obstacle as most international codes do not contain limitations and methods for the design of this type. The AASHTO LRFD gives some rules to design this CFST. Still, these limitations are for CFST without the deck slab; these limitations are considered very conservative. This study includes two parts experimental and theoretical. The experimental part consists of testing one specimen of the CFST composite beam, as shown in Figure 2.4. The ultimate load is 783.4 kN, and the corresponding deflection at mid-span is 95.5 mm; at this stage of load, the concrete is crushed under load. In the theoretical part, the bending capacity of this type is predicted based on full interaction between the concrete slab and steel tube (no-slip between concrete slab and steel tube).

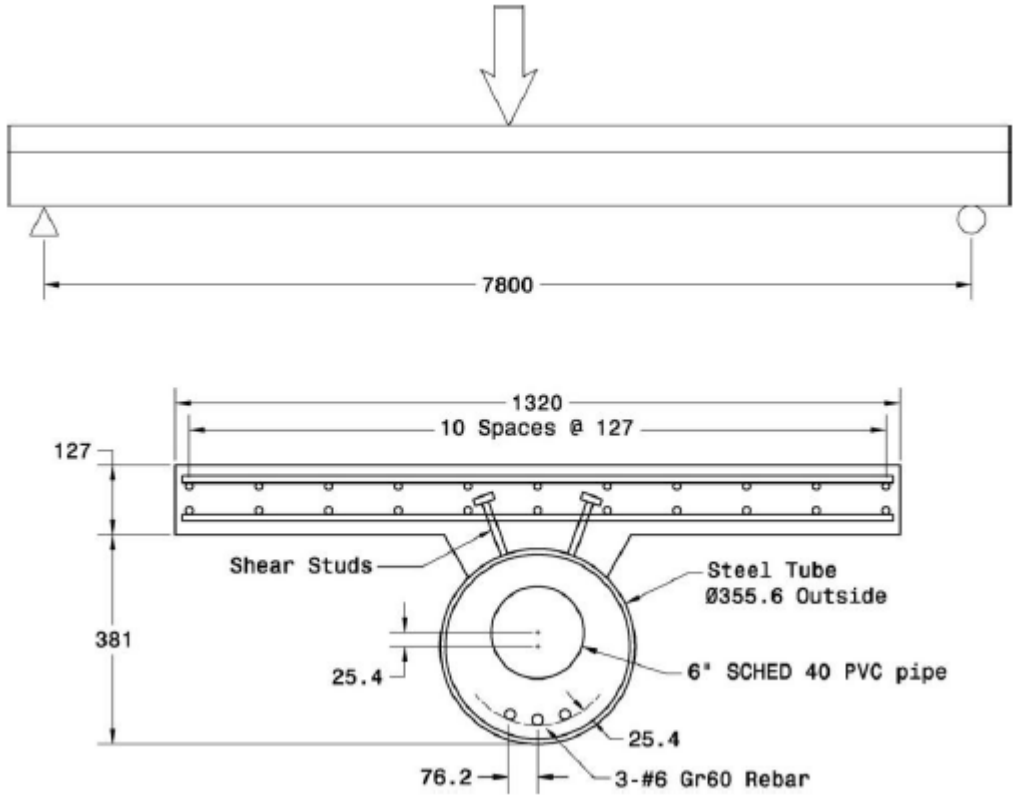

Figure 2.4 Loading and specimen details

Kang et al. [20] conducted two groups of tests. The first group included conducting tests for five specimens of steel tubes filled with concrete, and this group of tests had several parameters. The most important is the type of the filling material (NWC, air mortar) the effect of friction between the steel tube and concrete inside the steel tube. The second group included testing three specimens of steel tubes filled with concrete composite with a concrete slab. The specimens were continuous beams with two spans. The first specimen was hollow in the zone of the positive moment, the last two models were filled with air mortar, but they differed by adding mechanical interlock. The second specimen filled the area of the positive moment by air mortar without interlocking, while the last specimen filled with the same material with interlocking between steel tube and air mortar inside a steel tube. Figure 2.5 shows the specimen details. The following conclusions are the most important findings of this study. First, concrete use as a filling led to increasing the flexural moment capacity and stiffness of CFST. Using mechanical interaction causes increasing the interconnection between the steel tube and fill material, leading to more flexural strength of the members.

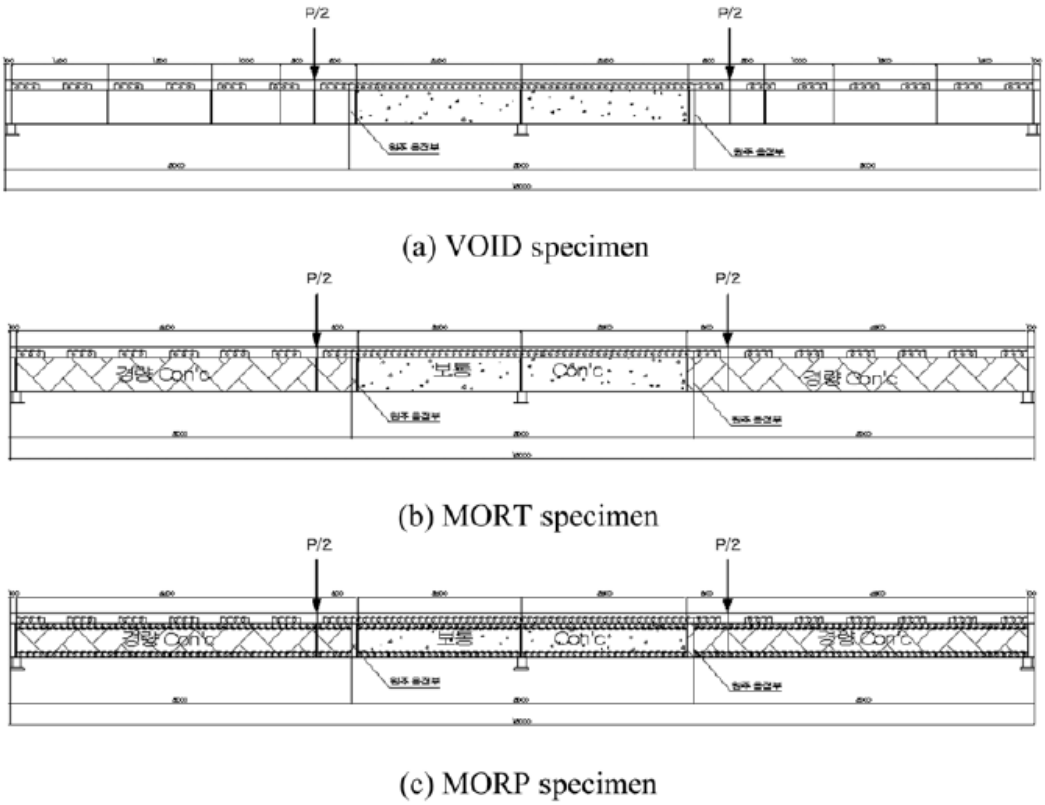

Figure 2.5 Loading and specimen details with mechanical interlock

Chin et al. [37] tested four specimens of a circular steel tube composite with a deck slab of six-meter in length. This study's major key was connecting two steel tubes to reach the final length of the specimen. The specimens were filled with concrete at the support zone, and the filling length was 1.6 meters from the support. This study used two types of connection (bolts and welding) to connect between the steel tubes. The reference specimen was fabricated from one steel tube with no contact. The connection made the other specimens of two steel tubes. The connection type of the second specimen was welding type, while bolts connected the last two specimens. The third specimen was made without filling the connection zone, while the last specimen used the bolts to fill the connection zone. Figure 2.6 illustrates the bolts connection of investigated specimen. The test results show that the connected specimens show similar stiffness and maximum moment capacity behavior compared with the reference specimen. In addition, the noise and vibration were decreased in the specimen filled by concrete in the connection zone compared with other specimens.

Figure 2.6 Bolt connections of specimen

Fu et al. [38] worked on the experimental and theoretical study of the CFST composite beam. The experimental study includes tests of one specimen only. Figure 2.7 and Table 2.1 show the test specimen details. The concrete type used for the slab is normal of 39.6 MPa strength, while the filled concrete in the steel is lightweight, 47.0 MPa. The parametric study includes a change in the size of the concrete slab and the steel tube wall. The authors concluded that the CFST composite beam has higher moment capacity and more ductility. The internal slip between the steel tube and the LWC inside the steel tube is assumed to be zero. The best section is when the ultimate load's neutral axis is located between the steel tube and concrete slab.

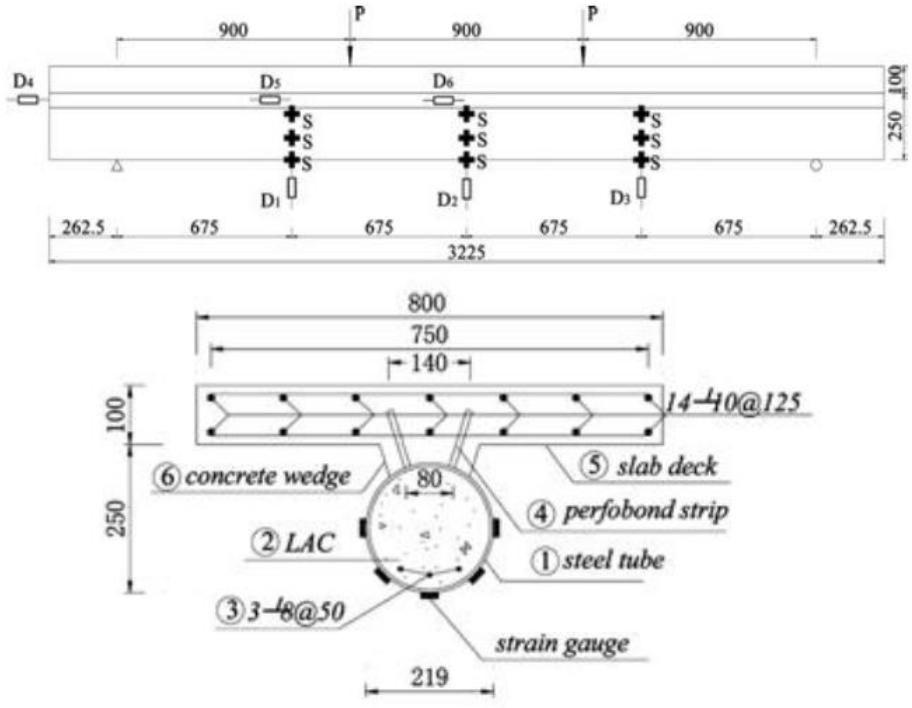

Figure 2.7 Details of specimen

Table 2.1 Details of specimen

component	Steel tube		Perfobond strip					Steel bar
	External diameter	Th	L	H	Th	Hole diameter	Hole distance	diameter
Detail	219	5.5	3175	100	10	12	125	10

Farhan and Shallal [39] studied the performance of composite CFST beams experimentally. The authors investigated nine specimens with many parameters such as specimen length, the effect of filling concrete inside steel tube, the effect of concrete compressive strength of slab, and the effect of steel tube section type (square, circular). The concrete type used to fill the steel tube was LWC. The load-deflection curve and load-slip curve were measured during the specimen test. The results show that the cracks reached the concrete slab when the load ranged from 50.9 % to 77.2 % of the ultimate load. The ultimate load decreased slightly when the compressive strength of the concrete slab was reduced. The slip at one-third of the specimen was more than the slip at the end of the specimen. The strength of the specimen has an empty steel tube decreased by 13.2 % compared with the reference specimen. Similarly, the initial stiffness and ductility of this specimen were lower than that of the reference specimen

2.4 Push Out for Perfobond Shear Connector

Hosain and Oguejiofort [40] studied the behavior of the perfobond shear connector. The main goal of the study finding the ultimate capacity of this type of shear connector by using the finite element technique. The equation estimated from the survey showed a good agreement compared to experimental studies.

Ahn et al. [41] studied the single and twin perfobond connectors. The study's main objective is to find the best method of ordering the perfobond connector and use it in the design and construction of the composite girder. The details of the test specimens are shown in Figure 2.8. Although the investigational results were related to some of the equations proposed by other studies, the results of the single perfobond connector were fewer than projected values. In contrast, the results of the double perfobond connector were overhead the projected values, so the equation was changed to match the investigational results of this type of perfobond connector.

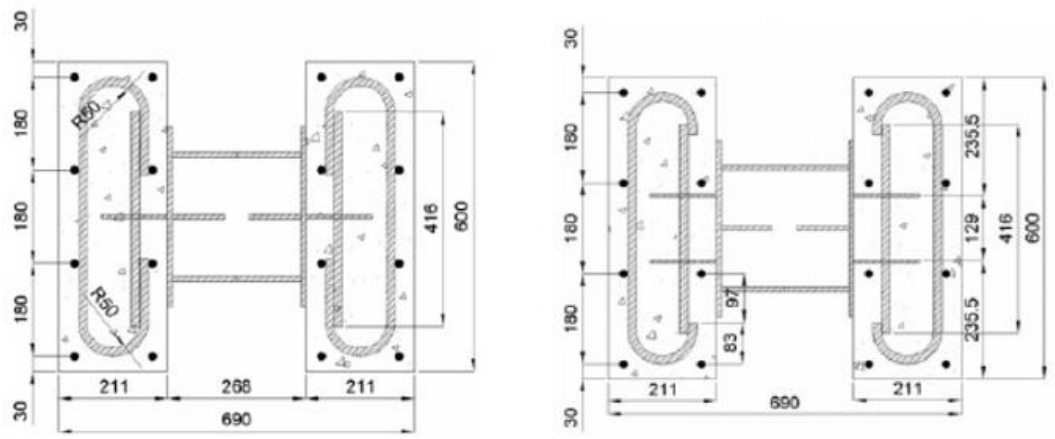

Specimen of the single perfobond.

Specimen of the twin perfobond.

Figure 2.8 Details for push out tested specimens

SU and Wang [42] tested a new perfobond shear connector known as a corrugated perfobond shear connector. The writers concluded that the performance of the corrugated connector is excellent; also, they found the load-slip curve for this type of shear connector. In addition, the shear volume of the crenelated connector was higher than the shear volume of the normal perfobond connector by 24%.

Zheng et al. [43] deliberated the perfobond shear connector. The study had two lines (investigational and mathematical). In the investigational program, the writers tested twenty-one specimens. The study aimed to find the ultimate shear capacity, failure mode, and slip behavior during the test. The second line of study includes numerical analysis of eighty-seven specimens. The theoretical research focused on concrete compressive strength and hole shape.

The authors suggested an equation to represent the behavior of the perfobond shear connector. This equation was based on hole size, concrete compressive strength, area of the transverse bar, and yield stress of the transverse bar.

Li et al. [44] examined the push out test experimentally and mathematically of wavy perfobond connectors. The findings show that many factors such as concrete compressive strength, the yield stress of transverse bar, the size of the hole, the wavy connector's area, and the horizontal estimate of the wavy perfobond shear connector.

Ibrahim et al. [45] carried out an experimental shear program of the push out test. The writers test twelve push out specimens divided into four groups. This study consists of three types of shear connectors (angle, stud, and perfobond connectors). The purpose of the study is to identify the behavior of the shear connector also find the stiffness and the shear strength of these types of shear connectors. The key outcomes were failure modes, shear strength, load-slip curve, connector stiffness, the shear volume of the perfobond connector greater than the shear volume of the stud, and angle connector.

Zheng et al. [46] studied the behavior of perfobond shear connectors. The experimental study included testing seventy-two specimens. The authors concluded that the push out test of the perfobond connector depends on many variables such as hole geometry, concrete compressive strength, concrete slab dimensions, arrangement of bars on the connector holes, and perfobond dimensions. Therefore, the authors suggested an equation to estimate the load-slip curve of the perfobond connector, including wide range parameters.

Zheng et al. [47] studied the performance of an alternative notched perfobond connector experimentally and numerically; one of the most advantages is to easy construction of perforating reinforcement bars. The experimental program included tests of six specimens, while the numerical program included analyzing forty-three samples. Finally, the authors suggested an analytical model calculate the shear strength capacity of this type of perfobond connector.

Zheng et al. [48] studied a new combined type (stud with perfobond connector) experimentally and numerically. Writers tested nine specimens in the investigational program. The goal of the investigational test was to compare the performance of the stud connector, perfobond connector, and the new mixed connector. The theoretical

study included additional variables such as connector dimensions and properties of materials. The results show that the shear strength of assorted connectors is subject to many such problems like transverse bar dimension, stud size, stud characteristics, hole size, concrete compressive strength, and properties of the transverse bar.

CHAPTER III

EXPERIMENTAL WORK

3.1 General

It is assumed that the concept of building with composite sections produces a structural resistance to the imposed loads more significant than the sum of the resistance of its parts. Therefore, CFST has been made since 1990 in China because of its structural advantages and artistic appearance [49]. A tri-axle compression state can be produced because of confinements of the infill that increase its strains and strength capacity [50,51] even when it is crashed. AISC [52] allows for the increase of the usable infill concrete stress to 0.95f ′c. Moreover, this confine delays the degrading in the strength, which leads to improved ductility [53].

Furthermore, the infill materials resist the local buckling of the steel tube [54]. Hosaka and his co-authors [55] reported more benefits that could be obtained from using CFST, such as reducing the noise induced by the traffic vibration. Although many experimental and modeling has been conducted to investigate the flexural behavior of the CFST, however, it is still hard to give a suitable explanation that can be generalized, and the problem was still on the table. Thus, it is essential to thoroughly understand the structural behavior of CFST because of their wide use in construction. It is worthy of mentioning here that there is a real difference between the CFST component and Steel Tube Composite Beams (STCB) because of the reinforced concrete slab that connects to the beam by a shear connector that should be considered. Including slab in STCB will complicate the problem; this complexity will increase with the number of parts that make up the composed member. Because the behavior stages depend on the different materials' properties, like the interaction between these materials, this interaction is based on the connection types. In this study, the structural behavior of the STCB was investigated. Two main investigated parameters were the

effect of the beam section aspect ratio (width/depth) and the slab thickness. This chapter deals with experimental work, including construction method, materials properties, curing conditions, and test setup.

3.2 The material used for test specimens

All the materials tests agreed with the ASTM. All materials and tests were conducted in Iraq at Al Nahreen University Engineering College Structural Laboratory.

3.2.1 Cement

For both mixes (lightweight and normal concrete), ordinary cement (type I) was used. Table 3.2 shows the cement chemical compounds, while the cement physical properties are displayed in Table 3.3. The cement properties comply with ASTM's provisions.

Table 3.1 Chemical composition of cement

Compound composition Result (%)	**Result (%)**	**Limitation**
Lime saturation factor	0.9	1.02-0.66
Tri-calcium		-
Sulfate content (SO3)	2.6	< 2.5 if C3A <5
		< 2.8 if C3A >5
Magnesium oxide (Mgo)	3.69	≤ 5.0%
Nonsalable substance	0.53	≤1.5
Loss of ignition	1.69	≤ 4.0

Table 3.2 Cement physical properties

Physical properties		**Result**	**ASTM**
Soundness, %		0.3	≤ 0.8
Setting time Initial, (minute) Final, (hours)		 120 3.01	 ≥ 45 ≤ 10
Fineness (Blaine), (m2/kg)		279	≥ 230
Compressive strength (MPa)	3days	15.1	≥ 15
	7days	37.72	≥ 23

3.2.2 Aggregates

3.2.2.1 Fine Aggregate

The sand used in this study was natural sand. Table 3.1 shows the grading method's sand results according to ASTM provisions. Figure 3.7 shows the actual sieve analysis. The results show that the obtained grading was within the limits of zone 1.

Table 3.3 Limitation and grading of sand

Sieve size (mm)	**Passing percentage (%)**	
	results	**Zone No III.**
9.5	100	9.5
4.75	96	4.75
2.36	88	2.36
1.18	65	1.18
0.6	29	0.6
0.3	10	0.3

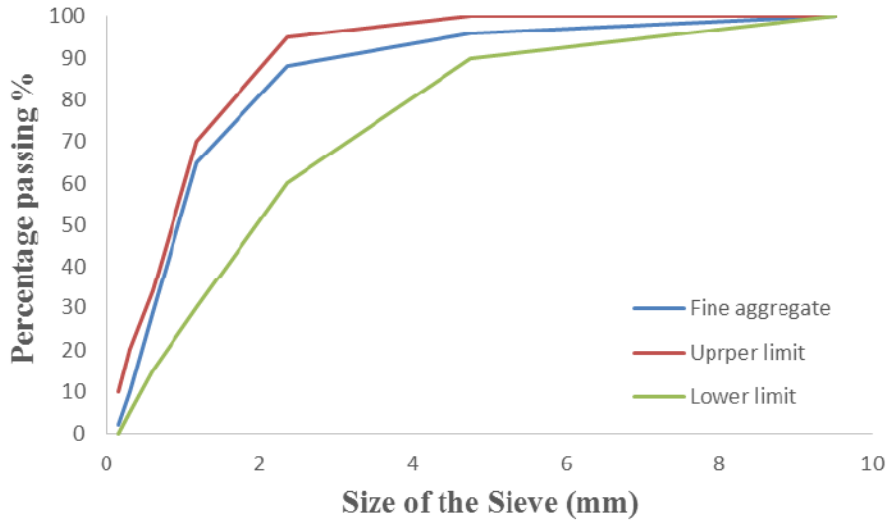

Figure 3.1 Sieve analysis of fine aggregate

3.2.2.2 Coarse Aggregate

Crushed gravel was used as a coarse aggregate. Next, the gravel was washed to remove the dust. Finally, the prepared gravel was stored in a saturated surface dry. Table 3.2 shows the gravel testing results. Figure 3.8 shows the actual sieve analysis.

Table 3.4 Gravel grading test results

Sieve size (mm)	Passing percentage (%)	
	Gravel	Limitations
14	100	14
9.5	98.66	9.5
4.75	3.66	4.75
2.36	0	2.36

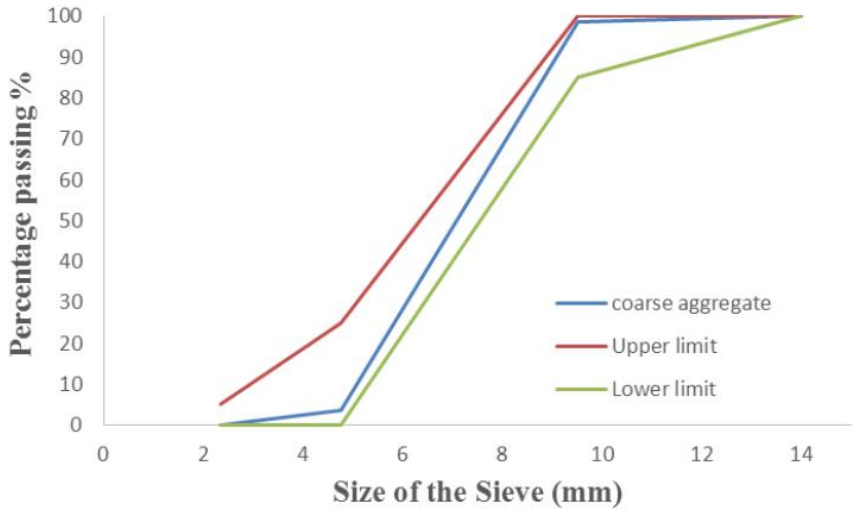

Figure 3.2 Coarse aggregate sieve analysis

3.2.2.3 Lightweight Coarse Aggregate

The lightweight coarse aggregate (LECA) is an unusual type of expanded clay that has been pelleted and laid-off in an exceedingly rotary oven at a very warmth. Because it is laid-off, the organic mixtures within the clay burn off, forcing the pellets to expand. The ensuing ceramic pellets measure lightweight, have high crushing resistance, and, thanks to its cellular structure, closed in a hard shell enhances the weight/resistance ratio. LECA is a natural product having neutral pH value and is sustainable. In addition, it has fire resistant, sound isolation, excellent workability, unchangeable resistance with time, and is natural environment-friendly. Figure 3.3 shows clay aggregate (LECA).

Figure 3.3 Clay aggregate (LECA)

3.2.3 Superplasticizer

High water reduction was used to decrease the water cement ratio required. The admixture ADVA- CAST-585 from GRSE Company Products was used to produce LWC NWC used to improve the workability of the fresh concrete. This Superplasticizer (SP) is classified as type G according to ASTM C494-17 [56]. The normal dosage for the ADVA-CAST-585 is between (130-780) ml per 100 kg cement from 1-3 percent cement weight.

3.2.4 Reinforcement Steel

The test method was done according to ASTM 996M-05 [57]. One steel reinforcement bar is used for all specimens (6 mm); this bar was used as longitudinal and transverse directions. This bar's yield stress (f_y) is 489 MPa, while the ultimate stress (f_u) is 579 MPa.

3.2.5 Steel plate used for tubes and perfobond connector

The test method was done according to ASTM 996M-05 [57]. The yield stress (f_y) was 425.6 MPa for the steel tube and perfobond plate. The maximum stress (f_u) was 525.43 MPa for the steel tube and perfobond plate, respectively. The steel tubes preparation was started by cutting the tubes in specific lengths as beams. Then, a perfobond connector was used to make a good connection between the concrete-filled steel tube and concrete deck slab. For all specimens, the cross-section of the perfobond connector is 50×4 mm, and cutting it with the same length of the specimens minus 5 cm from one side. After that, they were welded with a single bevel butt weld at the corners.

Before it welded the perfobond connectors, a-holes were made on it with a diameter of 7 mm repeated at 25 mm so the transverse reinforcing bars (6 mm) can be passed through it (i.e., normal to the connectors). Figure 3.4 shows the welding process of the steel tube and perfobond connector. After casting the LWC in the side steel tube, the steel tube was left for two weeks so as for the LWC to accumulate the specified hardening, as shown in Figure 3.6.

Figure 3.4 Welding process of steel tube

3.3 Mixing Procedures

3.3.1 Mixing of lightweight concrete

The LWC mixture contains clay aggregate LECA instead of normal gravel, this mix's design strength (f'_c) at 28 days is 15 MPa. Table 3.5 shows the materials and design mix of LWC according to ACI committee 211.2-98 [58].

The mixing drum should be clean and wet before starting the mixing process. Figure 3.5 is showing the mixer used in this work. According to the ACI committee (211.2-98) [58]. With the following steps (i), LECA was added to the mixer. (ii) Fine aggregate and cement were added to the mixer. (iii) Mixed the dry materials for 2 minutes. The speed of the mixer was 26 cycles per minute. (iv) Superplasticizers were added to water, then added to materials in the mixing drum during rotary the drum and mixed for two to three minutes.

Figure 3.5 Concrete mixer

Table 3.5 Details of the concrete mix design of LWC

Material	**(kg/m3)**
Cement	500
Sand	875
LECA Water (w/c =0.3)	250 150
SP (L/m3) (0.4 % of cement)	2

3.3.2 Mixing of Normal Concrete

The NWC was designed according to (ASTM C192/C192M-05) [59]; this mix's design strength (f'_c) at 28 days is 25 MPa. Table 3.6 shows the quantities of materials used in this mixture.

Table 3.6 Normal weight concrete mixture proportion

Material	**(kg/m3)**
Cement	400
Sand	750
gravel Water (w/c =0.4)	1100 132
SP (L/m3) (1 % of cement)	0.4

NWC was mixed according to ASTM C192/C192M-05 [59]. The mixing drum should be clean and wet before starting the mixing process. The procedure used to mix the batches is as follows (i) gravel was added to the mixer. (ii) Fine aggregate was added to the mixer. (iii) Mixed the dry materials for 2 minutes. The speed of the mixer was 26 cycles per minute. (iv) The Cement was added to the mixer. (v) Superplasticizer was added to water then added to materials in the mixing drum during rotary the drum and mixed for two to three minutes.

3.4 Casting and Curing Process

3.4.1 Casting lightweight concrete inside steel tubes

The total mixing time was about 5-10 minutes in this work. Next, the specimens were placed vertically and filled the steel tube from one end with LWC. Figure 3.6 shows casting the LWC in a side steel tube.

Three cylinders were taken (150 x 300) mm to test the compressive strength (f'_c) of concrete according to (BS1881-part1) [٦٠] and (3) cylinders (150x300 mm) were cast to evaluate the splitting tensile strength. The inside surfaces of all molds were prepared by putting oil to prevent adhesion with concrete after hardening. After 24 hours, all the cylinder specimens were taken off from their molds and submerged in the water basin for twenty–eight days, as shown in Figure 3.7.

Figure 3.6 Casting the LWC inside the steel tube

Figure 3.7 Molds after casting

3.4.2 Casting NWC and curing of decks slab

The formwork was placed horizontally to cast the composite beam's deck slab. Concrete was gradually put in the formwork, and a vibrator was used to remove the voids in the concrete, then the surface of the concrete was leveled. After 24 hours, all the specimens were taken off from their molds and submerged in the water basin for twenty–eight days. Figure 3.8 shows the casting of the concrete deck slab.

Figure 3.8 Casting of the concrete deck slab

From every mix, three cylinders were taken (150x300) mm to test the compressive strength (f'_c) for concrete according to (BS1881-part1) [٦٠], and (3) cylinders (150x300 mm) were cast to evaluate the splitting tensile strength.

3.5 Fresh Concrete Tests

The slump tests have been done to measure the fresh properties of NWC and LWC. According to the ASTM C 143/C 143M-2015 [٦١], a slump test of NWC and LWC has been done, as shown in Figure 3.9.

Figure 3.9 Slump test

3.6 Hardened Concrete Test

3.6.1 Compressive strength

The cylinder compressive concrete strength test was done according to (BS 1881-Part 1) [60]. Three cylinders (150×300 mm) for each concrete mix were tested. The instrument test is shown in Figure 3.10.

Figure 3.10 The compressive strength instrument

3.6.2 Splitting Tensile Strength

The tensile strength test was conducted in the same compression test machine according to ASTM C496 [62]. Three cylinders (150×300 mm) for each concrete mix were tested. The instrument testing is shown in Figure 3.11.

Figure 3.11 Splitting tensile strength test

3.7 Composite Beam Specimens

3.7.1 Steel tube composite T beams specimens

The flexural behavior of six specimens of STCB was investigated under one point loading test setup. Each specimen consists of two composite parts. The first part is the steel tube beam filled with LWC, and the second part is the deck slab. The details of tested specimens are shown in Figure 3.12. The two parts were connected using a perfobond-rib shear type connector of 50 × 4 mm and the specimens.

The main parameters investigated were the effect of the beam section aspect ratio (width/depth) and the slab thickness. Three used aspect ratios were (0.4, 0.5, and 0.6), where the beams' sizes were 80, 100, and 120 mm in width; for all beams, the thickness was 200 mm. Nomenclature (S0.4, S0.5, S0.6) the character S refers to specimens, and the numbers refer to the amount of aspect ratio with slab thickness 75 mm. Moreover, two slabs' thicknesses (85, 100 mm) were tested. It was nomenclature by (SL85, SL100) where the character L refers to slab, the number refers to slab thickness, and one specimen was hollow composite beam Control Specimen (CS).

The slabs were doubly reinforced with conventional diameter reinforcement (6 mm) in each direction. The reinforcement ratio was the same for all the specimens, where the longitudinal reinforcement ratio (ρ_{long}) was equal to 0.7 %, and the transverse reinforcement ratio (ρ_{trans}) was 0.6 %. Therefore the numbers of rebars were altered based on the slab thickness and width. The dimensions of the perfobond connector were 50x4 mm which was used as a shear connector between the steel tube and the deck slab, the bottom layer of transverse steel reinforcement passed through the perfobond plate with a hole of 7 mm. Figure 3.13 shows the connecting method. A Linear Variable Differential Transformer (LVDT) was attached beneath the steel tube at mid-span to investigate the displacement behavior.

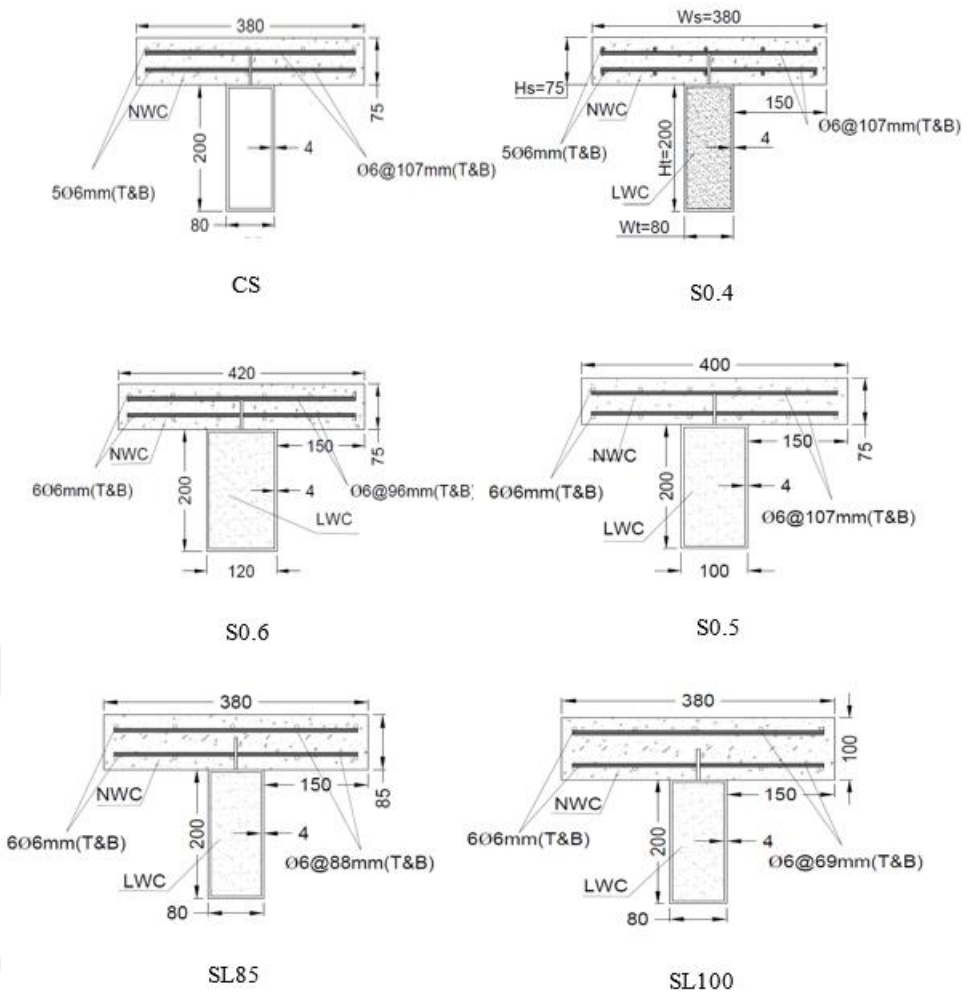

Figure 3.12 Scheme of the specimens STCB

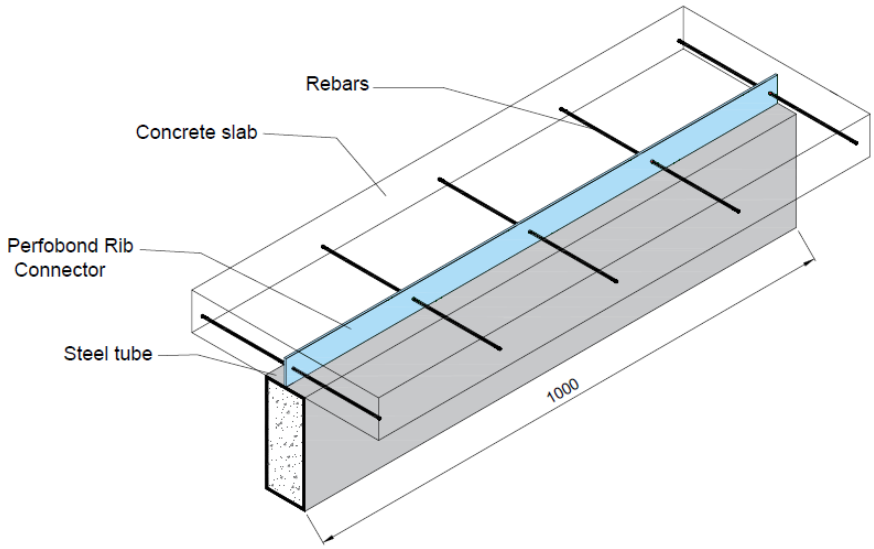

Figure 3.13 Perfobond connector

All specimens were tested under monotonically increasing load at mid-span of the slab; the tested sample was supported from the two edges by linear cylindrical steel support. Centric slip (δ_u) between the steel beam and the concrete slab was analyzed using LVDT installed at the center of the steel beam to investigate the displacement behavior of the different parts of a specimen,

The concrete of the deck slab was cast. The plywood formwork was used to cast the deck slab. These molds give clear dimensions for the slab model. Figure 3.14 shows the plywood formwork for the concrete slab. After finishing making the wooden formwork, the reinforcing steel bars were cut out and placed consistent with the size and details.

Figure 3.14 Casting the plywood formwork for the concrete slab

3.7.1.1 Test Setup of T beams specimens

All beam specimens are tested up to fail as a simply supported beam. All specimens were investigated using concentrated force applied at the middle of the composite beam. The moving part of the device was the upper part with a hydraulic jack. The lower part is fixed to a large stiff steel section. A Linear Variable Differential Transformer (LVDT) was attached beneath the steel tube at mid-span to investigate the displacement behavior. Figure 3.15 illustrates the test setup, longitudinal dimensions, and the locations of the LVDT.

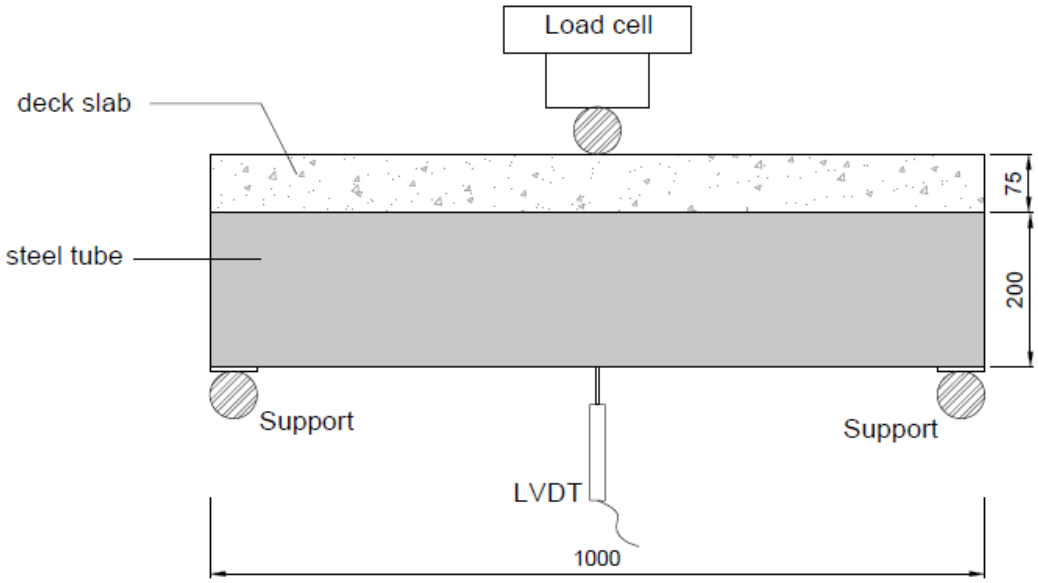

Figure 3.15 Test setup and locations of the LVDT

The composite beams were tested in a 2000 kN capacity testing machine. The load rate was 1 kN applied continuously until the specimen failure. Figure 3.16 shows the instruments used in the test of the specimens.

Figure 3.16 Hydraulic testing machine

3.7.2 H beams composite push out test specimens

Three specimens were prepared for the push out test; each specimen comprised three main parts, one steel beam and two reinforced concrete slabs of 500 mm length and

two different widths; the details of the specimens are listed in Table 3.7. The rectangular steel beam was fabricated from a mild steel sheet of 4mm thickness. The sheet was cut and then bent to form the two flanges of the beam and single web. A strip of length equal to the remaining web width was cut, then the two parts were tack welded with a single bevel butt weld. Ribs of 450 mm length and 50 mm width were welded to both sides at the center of the beam's flanges, six holes of 8 mm were punched to allow the transverse re-bars to pass through it. Two beams (R1 and R2) were infilled with LWC to mimic the loaded flexural members, while a reference beam (R0) was kept hollow, as shown in figure 3.17, the LWC was filled in layers that vibrated from in and outside via a poker vibrator.

The second and third parts of the push out test specimens were two slabs of NWC; both slab thicknesses were 75 mm for all specimens, while the slab width was varied (380 and 400 mm) based on the width of the beam′s flange. So the wings of 150 mm for each specimen were guaranteed. The length of the slabs was 500 mm. The three parts were connected, so a 50mm offset was earned between the slabs and the steel beam's ends. The slabs were reinforced with double layer conventional reinforcement of diameter 6 mm in each direction, as shown in Figure 3.18. The numbers of transverse and longitudinal re-bars were (6 and 5) respectively, the reinforcement was laid so that 15 mm concrete cover was obtained.

3.7.2.1 Test Setup of H beams specimens

The specimens of push out were supported by stiff area from the two edges of the slabs while the load was applied at the edge of the steel beam in monotonic increasing rate up to failure. Figure 3.19 shows the test setup and location of LVDT. The loading rate was 1 kN/sec via a loading machine of 200 ton-force capacities.

Table 3.7 The details of composite H beam specimens

Spec.	**Slab H_s=75**		**Tube H_t=200**			
	L_s	**W_s**	**L_t**	**W_t**	**Th**	**Fill**
R0	500	380	450	80	4	0
R1	500	380	450	80	4	LW
R2	500	400	450	100	4	LW

Figure 3.17 Hollow steel tube and typical composite H beam specimen

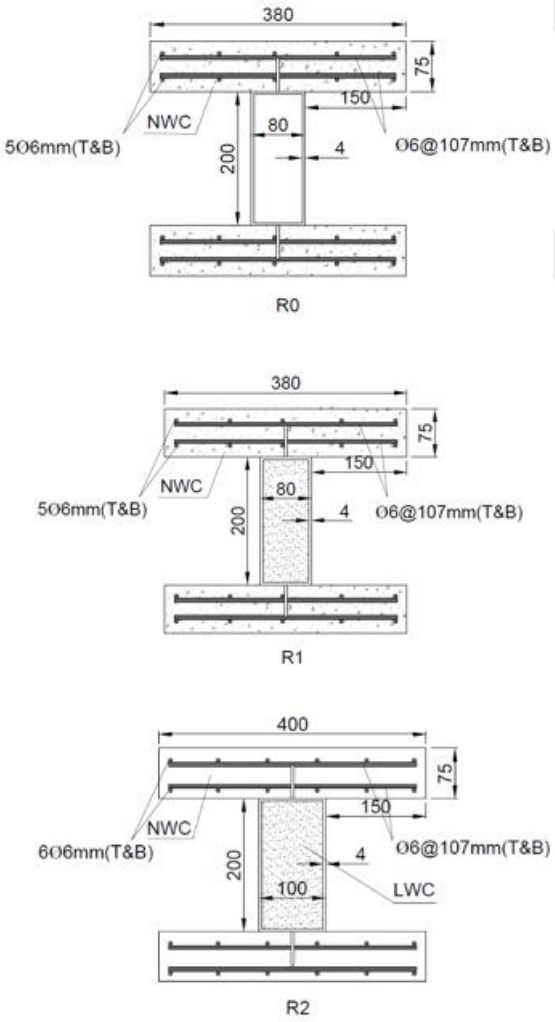

Figure 3.18 Details of composite H beams specimens

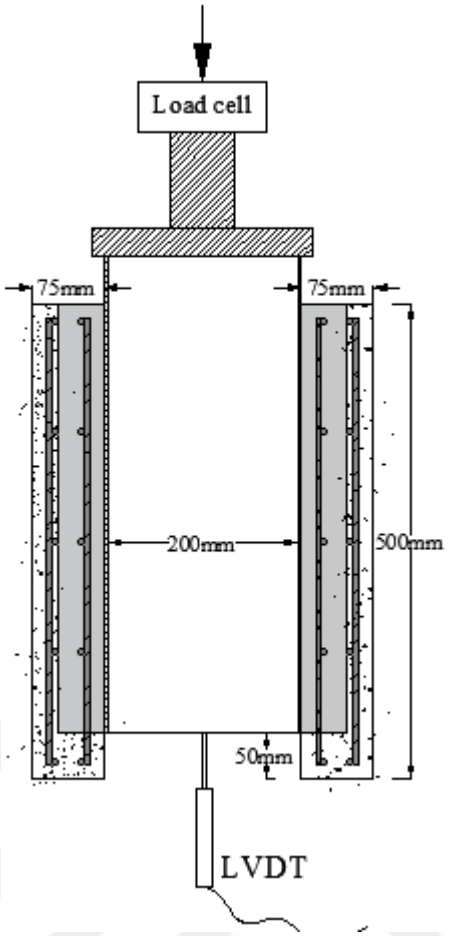

Figure 3.19 Test setup of H beams and location of LVDT

CHAPTER IV

EXPERIMENTAL RESULTS AND DISCUSSIONS

4.1 General

This chapter introduces the experimental results of a one-point flexural testing setup for six STCB. In addition to evaluating the mechanical properties of the concrete and steel used in this work, the shear strength of the connector (perfobond rib connector) was also checked based on the push out test method. The main parameters considered were the aspect ratio of the steel tube cross-section dimension, the slab thickness, and the effect of the filling concrete in the steel tube. The results were introduced into three parts. The first part focused on the mechanical properties of the materials used in this study (concrete and reinforcement bars strength). The second part provided the results of the behavior of the shear connector. Finally, in the third part, the structural behavior and ultimate strength of the STCB were introduced.

4.2 Mechanical properties of the materials

4.2.1 Compressive and tensile strength of concrete

The slump test was performed for both types of fresh concrete mixes according to ASTM C143/C. The results for the slump test are illustrated in Table 4.1. In addition, the compressive and tensile strength of the NWC and LWC concrete under standard test methods for cylinders of 150 × 300 mm dimensions are shown in Table 4.2.

Table 4.1 Slump test results

	NWC	**LWC**	**Limitation ASTM C 143/C**
Slump (cm)	12.8	12.7	2.5-17.5

Table 4.2 Compressive and tensile strength of concrete

	compressive strength (f'_c) (MPa)	**Tensile strength (f_{ct}) (MPa)**
NWC	27.2	2.0
LWC	19.2	1.4

The f'_c and fct were evaluated under the mentioned provisions; the ratio of fct to the f'_c depends upon the magnitude of the concrete strength. The higher f'_c, the higher f_{ct}, but the rate of increase of f_{ct} is of decreasing order. The f_{ct} of concrete is more sensitive to curing than the f'_c. The f'_c of the LWC was less than that of NWC by 29%. Moreover, the tensile strength of the LWC was less than that of NWC by 31%. The proportion of the $K = f_{ct} / \sqrt{f'_c}$ for LWC and NWC were 0.38 and 0.32, respectively.

The failure mode of the standard cylinders was investigated. It is found that the failure of cylinders under splitting load was due to the crashing of the lightweight aggregate for LWC, while the NWC cylinders were failed due to matrix cracking. The crack patterns of the cylinders confirmed this mode under uniaxial load, where the cylinders of LWC were damaged at the half that exposed directly to the moving machine plate; this means that the compression stress was slowly transformed from the contact surface to the middle of the cylinder. In contrast, the NWC cylinders are cracked approximately equally around the cylinders.

The differences in the mechanical properties between the LWC and NWC depend on many factors, rate and magnitude of the lightweight aggregate absorption is the main factor that affects the fresh and hardened concrete.

4.2.2 Steel strength

Three steel sections were used in the current work. The first was a plate of 4 mm used to fabricate the steel tubes. Moreover, the thickness of the same plate was used to manufacture the perfobond rib connectors of different holes. Finally, a steel bar of one diameter (6 mm) was used for reinforcing the concrete deck slab. Table 4.3 illustrate the yield and ultimate strength of the steel sections. The test was obeyed ASTM 996M-05 [57] provisions.

Table 4.3 Steel test results

Steel	Yield stress (MPa)	Ultimate strength (MPa)
Steel plate (4 mm)	426.6	526.4
Steel bar (Ø6 mm)	489.0	579.0

4.3 Results of steel tube composite T beams with concrete deck slab

4.3.1 Maximum load resistance and load-deflection

Table 4.4 shows the load resistance of the STCBs' used in the current work. Filling the steel beam by LWC significantly increased the STCB ultimate resistance. The ultimate resistance (P_u) of the S0.4 was more significant than the P_u of the reference spaceman CS by 90.71 %, while the deflection increased by 208.04 %. Furlong [6٣] found that the strength capacity from hollow steel tubes alone is about 49 % lower than that filled one; this means that the slab connected to the beam was improved the strength of the hollow STCB. Moreover, increasing the slab thickness by 13.33 % (S0.5) led to a decrease of 18.29 % compared to reference specimen S0.4. Still, the specimen does not affect the deflection compared to the specimen S0.4, while increasing the slab thickness by 30% was increased P_u by ٦,٩٦%, with a 39% decrease in deflection.

Table 4.4 Result of the tested tube composite T beams

Beam	type	Pcr (kN)	δcr (mm)	Pu (kN)	Increasing of Pu %	δu (mm)
CS	hollow	119	7.38	169.60	-	10.94
S0.4	filled	120	5.64	323.45	90.71	33.70
S0.5	filled	189	11.12	297.33	-18.29	34.75
S0.6	filled	120	5.29	176.41	-45.45	8.77
SL85	filled	170	8.25	255.89	-20.88	20.15
SL100	filled	164	6.95	342.75	6.96	20.50

The load-deflection curves for all STCB used in the current work are depicted in Fig. 4.1. It is seen that the curves generally have four main stages before they fail and many sub-stages; these stages are illustrated in Figure 4.2. All stages result from the varied structural materials (the reinforcement steel bars, the NWC, the steel tube, and the LWC). Therefore, the final load-deflection behavior of the STCBs is affected by many

factors, which is provide high restraints, imposing the resistance and the displacement value, such as the slab thickness, the steel tube dimensions, the interaction between the slab, the tube (connection and the friction). Besides the inclusion of filled materials. In the current work, all factors are kept the same for all STCBs, except the slab thickness and filled LWC.

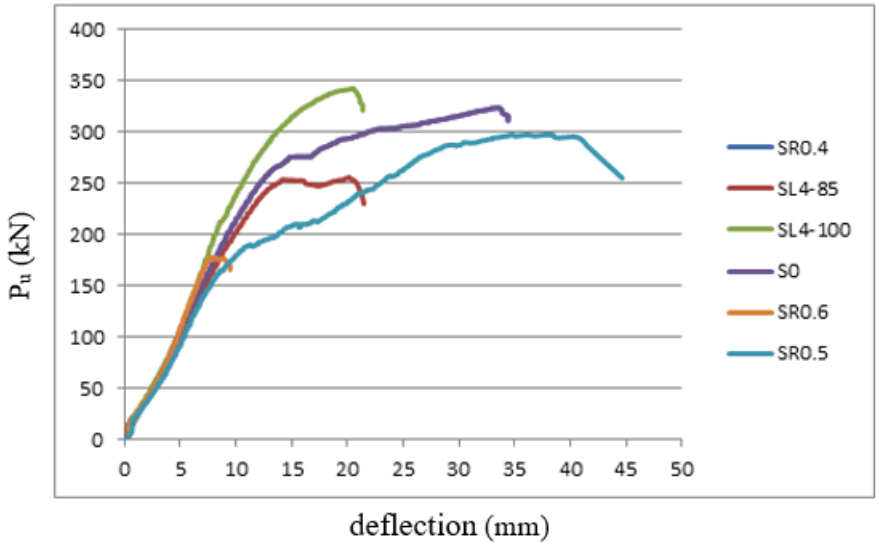

Figure 4.1 Load-deflection curves of all composite T beams

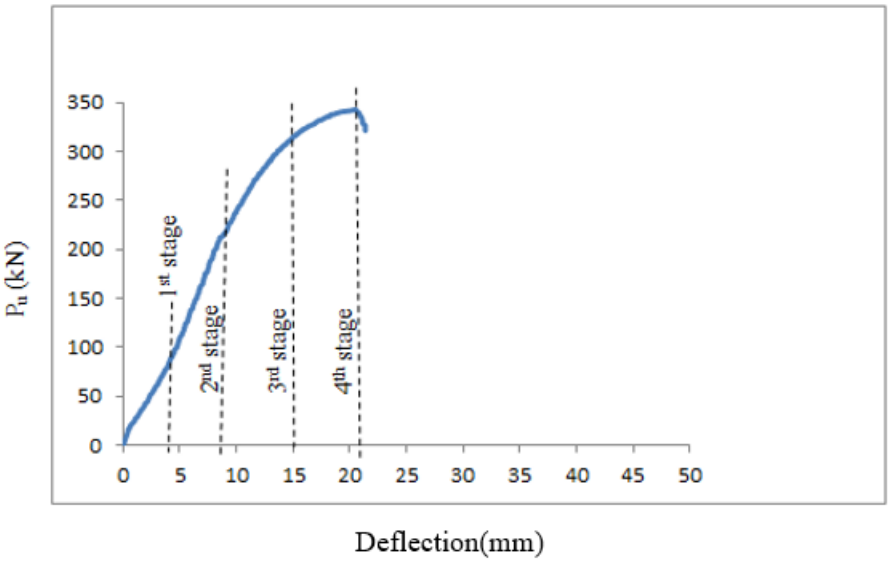

Figure 4.2 Typical load-deflection stages

Generally, the produced stages can be introduced as follows: the first stage is the uncracked elastic behavior; in this stage, the stresses transform ideally along the compression strut of the concrete slab from the loading point to the supports. Therefore all curves were identical. It is worth mentioning that the values of the Pu are limited

to the slab and beam resistance simultaneously, i.e., there are sub-stages based on the strain of the fibers (for slab and beam) under high stress so that a bilinear strain can be expected. The steel beam work as elastic support to the middle portion (strip) of the slab, while the strain of the two wings kept the same as in the middle strip, and this led to an increase in the flexural moment capacity and the ductility of the concrete slab compared to the same slab without beam support. In the second stage, NWC was cracking and still on elastic deflection behavior; nevertheless, some NWC was still in the uncracked-elastic stage. In this stage, the curves start to separate with different increment rates, where the increment rate decreases compared to the CS.

Moreover, this rate decreases with increasing slab thickness so that the slab thickness and filling the beam have a significant effect on STCB deflection behavior. At the same time, stress increases on the steel tube lower flange and lower fiber of the slab in different amounts. In the third stage, the load-deflection curve is still almost linear. However, NWC is in the elastic cracking stage while the strain of the beam's lower flange has increased, which leads to cracking the LWC. Han [10] found that the inelastic stage for steel-filled tubes starts at 20% of the ultimate moment capacity, while the STCB used in this stage begins at high percentages reach 80 %, which means that composed of the two parts increased the elastic zone.

Finally, in the fourth stage, the load-deflection relation exhibited a nonlinear form with variable plateau, where SL85 and SL100 showed a significant deflection plateau compared to CS and S0.4, which showed sudden failure.

4.3.2 Failure mode

After tasting, all specimens were investigated visually, many types of failure were found. Buckling at the support in the steel beam was recognized in CS, while shear & flexural cracks at the slab were recognized in CS and SL85. Pure flexural cracks in a few numbers were identified in S0.4 and SL100. However, connection failure at the intersection between the slab & beam was seen in the specimen with high slab thickness (SL85 and SL100). It is worth mentioning here the multi cracks produced in S4-85 indicate the ductility characteristic. Moreover, local cracks were recognized in the core of the beam of SL85 and SL100, and this is not surprising because high applied load buckles the steel plate that transfers the load to the low strength LWC in the core. Figures 4.3 and 4.4 show the cracks of specimens.

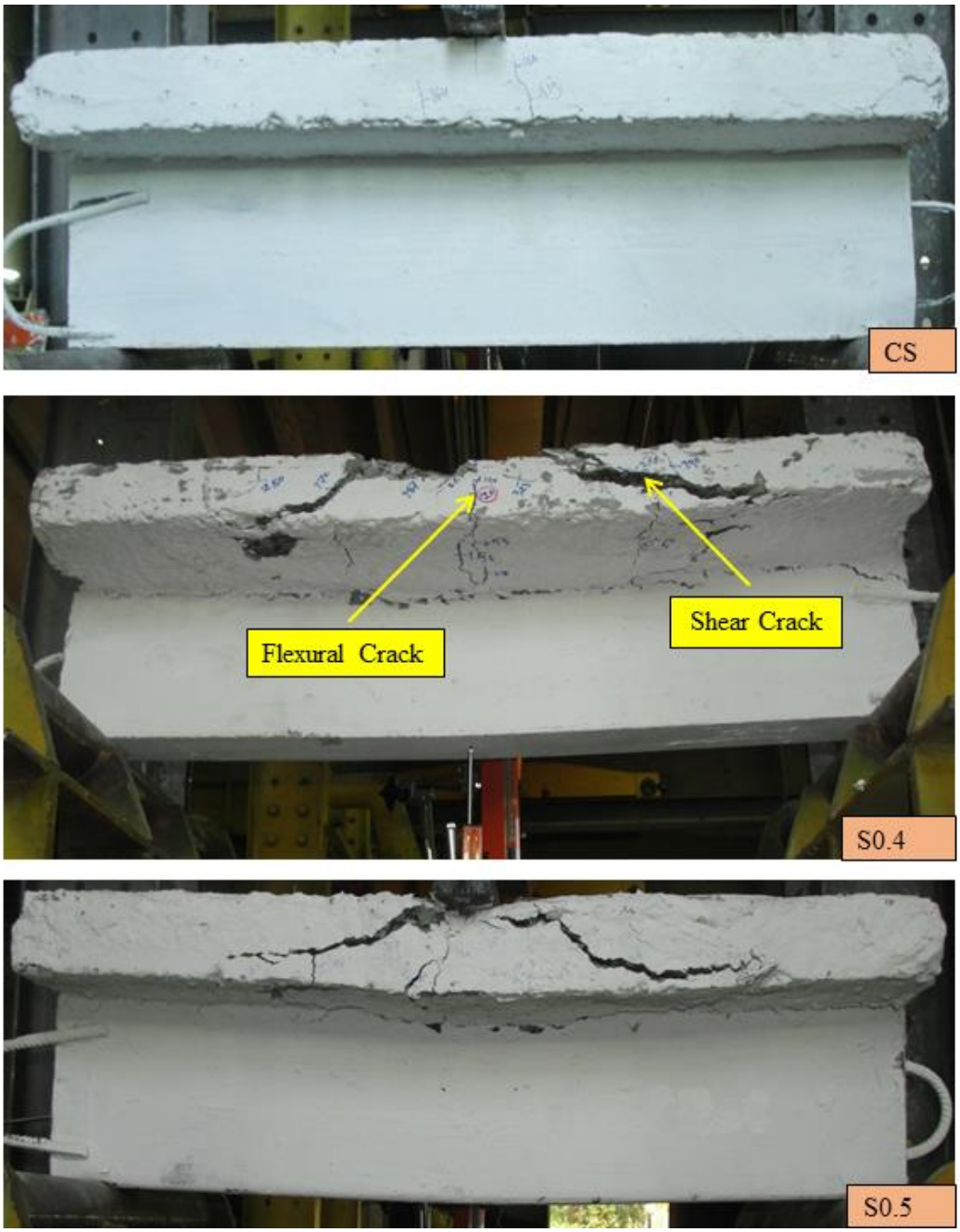

Figure 4.3 Cracks for the testing specimens

Figure 4.4 Cracks for the testing specimens

4.4 Push out Test Results of composite H beams

4.4.1 Push out strength

The push out specimens' shear strength (P_u) was tested in a universal machine of 200 ton-force capacity. Because estimating the ultimate shear strength of the Perfobond rib is difficult [6ٔ], monotonic loads were applied up to failure. Centric slip (δ_u) between the steel beam and the concrete slab was investigated using LVDT installed at the center of the steel beam.

The experimental results showed a significant effect of the infilled concrete in the beams. Comparing the strength of push out between the hollow beams (R0) and the filled specimen (R1) showed an increase in the shear strength by 14%. Although the contact area increased 25 % in R2, the surprising results were the decay in the shear strength compared to R1, and the decay was 21 %.

Many equations were proposed to estimate the push out perfobond rib's shear strength. Oguejiofor and Hosain [6◦] assumed that the strength depends on the effect of reinforced concrete slabs, the effect of the properties of the transverse bars, and the effect of dowel action of the holes. They proposed Equation 4.1. It is shown that the calculated strength due to Equation 4.1 was optimistic higher than the experimental strength in the current work by seven times, this is because the two terms in Equation 4.1 assumed that the spalling is resisted by the whole portion of concrete that is overestimated.

$$Q = 0.59\, A_c \sqrt{f_c'} + 1.233\, A_{SX}\, f_y + 2.871\, n d_{rib}^2 \sqrt{f_c'} \tag{4.1}$$

Therefore, Oguejiofor and Hosain [40] revised the first term in Equation 4.2, the spalling resistance was considered, and the effect of rib dimensions was included. As depicted in Equation 4.2.

$$Q = 4.5\, h_{rib}\ t_{rib}\, f_c' + 0.91\, A_{SX}\, f_y + 3.31\, n d_{rib}^2 \sqrt{f_c'} \tag{4.2}$$

Yoshitaka et al. [66] compared the effect of increasing the rib thickness. They found that two different failures can happen in the steel strip area; a tension failure can occur for a then strip, while a shear failure can occur in specimens with thick stripes. They introduced their equation (Equation 4.3) on these two assumptions.

$$Q = 1.45\left[(d_{rib}^2 - d_b^2) f_c' + d_b^2\, f_y\right] - 26.1 \tag{4.3}$$

Sara and Bahram [67] proposed Equation 4.4 that included the effect of the interface area as an additional parameter to Equation 4.2. Moreover, a significant modification was applied to the other terms.

$$Q = 0.747 H_{slab}\, h_{esc} \sqrt{f_c'} 0.413\, b_{beam}\, L_c + 1.66\, n\pi \sqrt{f_c'} \left(\frac{d_{rib}}{2}\right)^2 + 0.9\, A_{SX}\, f_y \quad (4.4)$$

Where; Q is the shear capacity at the shear connector (N), $f_c^{'}$ is the compressive concrete strength (MPa). A_c is the shear area of the concrete slab (mm2). A_{sx} is the area of the transverse rebars in the rib holes (mm2), f_y is the yield strength of the transverse rebar (MPa), n is the number of rib holes, d_{rib} is the diameter of the rib hole (mm), h_{rib} is the height of the rib (mm). t_{rib} is the thickness of the rib (mm), d_b is the bar diameter (mm), L_c is the contact length between the concrete slab and the steel beam flange (mm). A push out test method assesses the behavior of the shear connector. The forces proposed to control the connector are concrete end-bearing resistance, dowel action, and transverse rebars in the rib holes [64].

The shear strength of the perfobond connector was calculated according to equations listed in Section 4.2 that were found in the literature. It is deemed appropriate to say that the mentioned equations 4.1, 4.2, and 4.3 were highly optimistic. In contrast, Equation 4.4 was pessimistic and underestimated the ultimate shear strength limited to the result of the current work. In addition, the effect of infill concrete and the interface between concrete and beam were not considered in the first three equations, while the infill effect is missing Equation 4.4 so that the local buckling of the steel beam is omitted. Table 4.5 compares the test results with the predicted shear strength found in the literature.

Table 4.5 Test results' and predicted shear strength found in literature

Specimen	**Current study P_{Exp} (kN)**	**$P_{Eq.1}$ [64] (kN)**	**$P_{Eq.2}$ [65] (kN)**	**$P_{Eq.3}$ [40] (kN)**	**$P_{Eq.4}$ [67] (kN)**	**δ_u (mm)**
R0	186.6	954	1037	580	107	9.2
R1	212.8	954	1037	580	107	14.8
R2	167.0	954	1037	580	107	16.3

4.4.2 Failure mode

Chug et al. [68] reported three failure modes of the push out specimens that can be categorized. The first is related to the shear connector. This failure can occur due to

the small size of connectors and the large size and strength of concrete. The second failure occurs due to low concrete strength, while the third failure can occur due to a quasi balance between concrete strength and rib size. For perfobond connectors, the second mode is standard, and this is because the contact area is wider than in other shear connectors. According to the test conducted in the current work, the perfobond rib shear connectors showed the second failure mode, which is the failure of the concrete slab. Representative crack patterns are shown in Figure 4.5 R1 and R2 show longitudinal cracks along with the slab up to 400 mm.

In contrast, shear cracks occur from the end of the connector forward to the end of the slab. These cracks were developed due to high shear stresses that transferred from the slab center at 50mm from the end to the two supports. The hollow beam R0 has different cracks, and no longitudinal cracks have appeared. However, inclined bearing cracks at the area above the supports were another crack that developed due to high stress at supports.

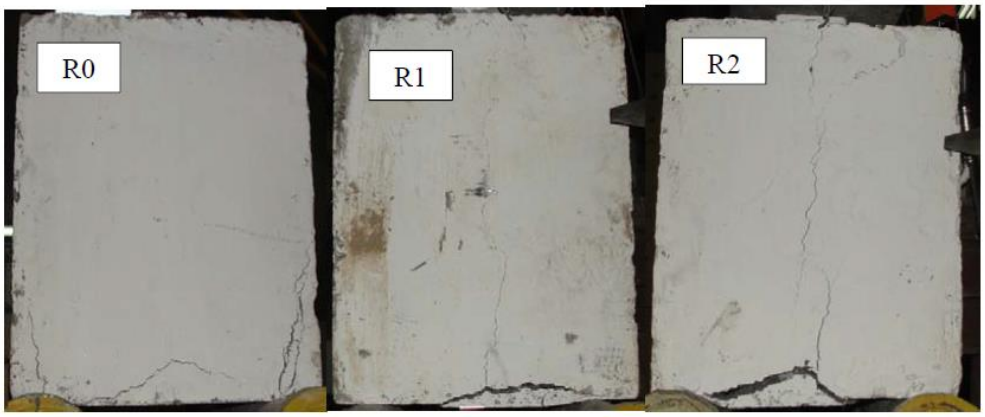

Figure 4.5 Crack pattern

4.4.3 Load slip relation

The relation between the applied load and the slip was investigated; the results showed that all specimens were failed suddenly after reaching the ultimate strength. Before peak strength, there were three stages because the specimens comprised many parts that failed sequentially. However, all specimens behave elastically up to 24 %, 55 %, and 21 % of ultimate shear strength of R0, R1, and R2, and this is because the small concrete dowel still resists the shear stress induced by the applied load. The concrete dowel resistance is relatively small and limited by concrete strength, and hence, losing

this action increased the slip rate under load used. Meanwhile, shear stress and a moment along the steel-concrete interface were induced. Different load transferring at the ends of the two edges of the beam flanges were developed, the strut stresses at this point increased, and the cracks were spread toward the supports, as well provided new increment slip rate, this rate depending on the concrete strength too. Increasing the interface area negatively acted on the load-slip curve where R2 shows separation in the curve with a short plateau. However, R2 was more ductile than the other two specimens. Figure 4.6 shows the Load-slip relation of the push out tested specimen.

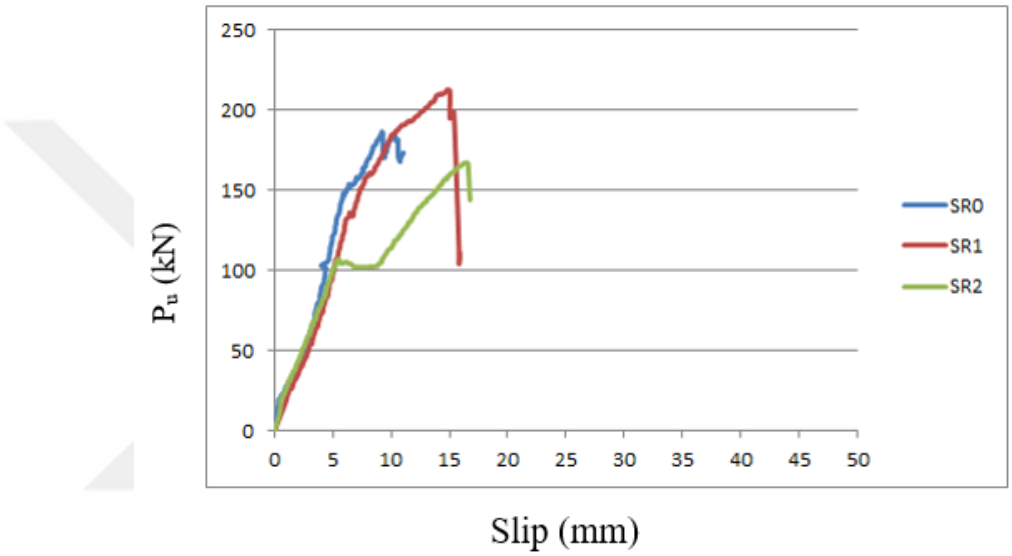

Figure 4.6 Load-slip relation of the push out tested composite H beams

CHAPTER V

CONCLUSION AND RECOMMENDATION

5.1 Conclusions

Based on experimental work and comparison, the following conclusions can be drawn limited to the current paper;

Beams in the push out test model infilled with concrete significantly improved the shear strength and the ductility behavior compared to the hollow beam. However, increasing the load resistance and ductility are followed by a high chance to segregate the two parts. Therefore, the shear connector is essential in resisting the high shear production in the interface between the slab and beam.

The most common failures in push out tests with perfobond ribs connectors are longitudinal shear cracks, end tension cracks, and local cracks at the supports. All failures are due to the concrete bearing.

Increasing the interface area between concrete and beams flanges negatively affected the ultimate strength of the push out specimen if other parameters were not adequately chosen.

Filling the beams with concrete significantly improves the ductility behavior. This improvement is based on many factors; the essential element is proportional of the slab thickness to the cross-sectional size of the beam.

Composing the steel-filled tube with reinforced slab improved the load resistance compared to the sum of the resistance of these parts, up to 11 % for hollow beams and 60 % for filled beams.

Filling the beams with concrete materials reduces local buckling in the area where the load is concentrated.

Increasing the load resistance and ductility is followed by a high chance of segregating the two parts. Therefore, the shear connector plays an important role in resisting the high shear production in the intersection between the slab and beam.

5.2 Recommendations for future research

1. Studying the performance of the STCB with concrete slab exposed to impact or dynamic load.

2. Studying the performance of the STCB with a concrete slab when using steel fiber in the concrete slab.

3. Studying the performance of the STCB with concrete slab exposed to repeated loading.

4. Studying the performance of the continuous STCB.

REFERENCES

[1] Chen, B.C., Wang, T. L. (2009).Overview of concrete filled steel tube arch bridges in China. *Practice periodical on structural design and construction*, **14(2)**, 70-80.

[2] Liu Y., L. Guo, Z. Li. (2018). Flexural behavior of steel-concrete composite beams with U-shaped steel girders, *in Proceedings 12th international conference on Advances in Steel-Concrete Composite Structures*. ASCCS 2018.

[3] Derysz J., Paweł. M. Lewiński, P. P. Więch, (2017). New Concept of Composite Steel-reinforced Concrete Floor Slab in the Light of Computational Model and Experimental Research, *Procedia Eng.*, vol. 193, pp. **168–175**.

[4] Ștefan-Marius (2019). Advanced Analysis Of Steel-Concrete Composite Structures by BURU.

[5] Han, L. H., Liao, F. Y., Tao, Z., Hong, Z. (2009). Performance of concrete filled steel tube reinforced concrete columns subjected to cyclic bending. *Journal of Constructional Steel Research*, **65(8-9)**, 1607-1616.

[6] Al Zand, A. W., Badaruzzaman, W. H. W., Mutalib, A. A., Hilo, S. J. (2018). Flexural behavior of CFST beams partially strengthened with unidirectional CFRP sheets: experimental and theoretical study. *Journal of Composites for Construction*, **22(4)**, 04018018.

[7] Fujikura, S., Bruneau, M. (2012). Dynamic analysis of multihazard-resistant bridge piers having concrete-filled steel tube under blast loading. *Journal of Bridge Engineering*, **17(2)**, 249-258.

[8] Kvedaras, A. K., Šaučiuvėnas, G., Komka, A., Juozapaitis, A. (2016). Design of circular composite beams with a different concrete core considering the effect of concrete in tension. J*ournal of civil engineering and management*, **22(1)**, 118-123.

[9] Elchalakani, M., Zhao, X. L., Grzebieta, R. H. (2001). Concrete-filled circular steel tubes subjected to pure bending. *Journal of constructional steel research*, **57(11)**, 1141-1168.

[10] Nakamura, S. I., Momiyama, Y., Hosaka, T., Homma, K. (2002). New technologies of steel/concrete composite bridges. *Journal of Constructional Steel Research*, **58(1)**, 99-130.

[11] J. Webb, J. J. Peyton, (1990) Composite Concrete Filled Steel Tube Columns. *Second Natl. Struct. Eng. Conf.* 1990 Prepr. Pap., p. **181**.

[12] Flor, J. M., Fakury, R. H., Caldas, R. B., Rodrigues, F. C., Araújo, A. H. M. (2017). Experimental study on the flexural behavior of large-scale rectangular concrete-filled steel tubular beams. *Revista IBRACON de Estruturas e Materiais*. **10**, 895-905.

[13] Gore V. D. Kumbhar (2015).Performance of Concrete Filled Steel Tube (CFST) Section: A Review. Int. *J. Sci. Res. IJSR*, vol. 4, no. 11, pp. **645–647**, Nov.

[14] Han, L. H., Li, W., Bjorhovde, R. (2014). Developments and advanced applications of concrete-filled steel tubular (CFST) structures members. *Journal of constructional steel research*, 100, **211-228**.

[15] An, Y. F., Han, L. H., Roeder, C. (2014). Flexural performance of concrete encased concrete-filled steel tubes. *Magazine of Concrete Research*, **66(5)**, 249-267.

[16] Kons Building: innovative steel-composite solutions for a complex inner citylocation(2020).https://constructalia.arcelormittal.com/en/case_study_gallery/luxembourg/kons_building_innovative_steel_composite_solutions. **10/06/2021**

[17] Composite Bridges Design & Construction(2020):. http://www.steelbridges.com/composite-beam-bridge.html. **08/06/2021**

[18] Cho J., J. Moon, H.-J. Ko, H.-E. Lee. (2018). Flexural strength evaluation of concrete filled steel tube (CFST) composite girder. *J. Constr. Steel Res.*, vol. 151, pp. **12–24**, Dec.

[19] Shariati, A., RamliSulong, N. H., Shariati, M. (2012). Various types of shear connectors in composite structures. A review. *International journal of physical sciences*. **7(22)**, 2876-2890.

[20] Kang, J. Y., Choi, E. S., Chin, W. J., Lee, J. W. (2007). Flexural behavior of concrete-filled steel tube members and its application. *Steel Structures*, **7(4)**, 319-324.

[21] J. Moon, C. Roeder, H.-E. Lee (2013, Dec.). Strength of Circular Concrete-Filled Tubes with and without Internal Reinforcement under Combined Loading. *J. Struct. Eng.*, vol. 139, p. **04013012**.

[22] Zhong-qiu, F., Bo-hai, J., Lei, L., Wen-jie, Z. (2011). Behavior of lightweight aggregate concrete filled steel tubular slender columns under axial compression. *ISSN 1816-112X*, **144**.

[23] Zhong, S.T. (1994). Concrete Filled Steel Tube Structures. *Heilongjiang Science and Technology Publishing House*, pp. **72–74**, pp. **260-308**.

[24] Zhong S., S. Zhang,(1999) Application and development of concrete-filled steel tubes (CFST) in high rise buildings. *Adv. Struct. Eng.*, vol. 2, no. 2, pp. **149–159**.

[25] Kloppel, V. K., Goder, W. (1957). An investigation of the load carrying capacity of concrete-filled steel tubes and development of design formula. *Der Stahlbau*, **26(1)**, 1-10.

[26] Nishiyama. (2002). Summary of research on concrete-filled structural steel tube column system carried out under the US-Japan cooperative research program on composite and hybrid structures. *Building Research Inst*.

[27] Kim D. K. (2005). A database for composite columns. *Georgia Institute of Technology*, p. **282**.

[28] Gourley B. C., C. Tort, M. D. Denavit, P. H. Schiller, J. F. Hajjar, (2008). A synopsis of studies of the monotonic and cyclic behavior of concrete-filled steel tube members, connections, and frames. *Newmark Structural Engineering Laboratory. University of Illinois at Urbana*.

[29] Hajjar J. F., B. C. Gourley, C. Tort, M. D. Denavit, P. H. Schiller, N. L. Mundis, (2013). Steel-concrete composite structural systems. *Dep. Civ. Environ. Eng. Northeast. Univ.*

[30] Lai Z., A. H. Varma, (2015). Noncompact and slender circular CFT members: Experimental database, analysis, and design, *J. Constr. Steel Res.*, vol. 106, pp. **220–233**.

[31] L.-H. Han,.(2004). Flexural behaviour of concrete-filled steel tubes. *J. Constr. Steel Res.*, vol. 60, no. 2, pp. **313–337**.

[32] Han L.-H., H. Lu, G.-H. Yao, F.-Y. Liao. (2006). Further study on the flexural behaviour of concrete-filled steel tubes. *J. Constr. Steel Res.*, vol. 62, no. 6, pp. **554–565**.

[33] Lu H., L.-H. Han, X.-L. Zhao. (2009). Analytical behavior of circular concrete-filled thin-walled steel tubes subjected to bending. *Thin-Walled Struct.*, vol. 47, no. 3, pp. **346–358**.

[34] Flor J. M., R. H. Fakury, R. B. Caldas, F. C. Rodrigues, A. H. M. Araújo. (2017). Experimental study on the flexural behavior of large-scale rectangular concrete-filled steel tubular beams. Rev. *IBRACON Estruturas e Mater.*, vol. 10, no. 4, pp. **895–905**.

[35] Hosaka T., T. Umehara, S. Nakamura, K. Nishiumi (1997, Sep.). Design and experiments on a new railway bridge system using concrete filled steel pipes. in Composite constructive-conventional and innovative (Innsbruck, 16-18), 1997, pp. **367–372**

[36] Mossahebi N., A. Yakel, A. Azizinamini. (2005). Experimental investigation of a bridge girder made of steel tube filled with concrete. *J. Constr. Steel Res.*, vol. 61, no. 3, pp. **371–386**,.

[37] W. J. Chin, J. Y. Kang, E. S. Choi, J. W. Lee. (2008). Study on structural behavior characteristics of concrete filled steel tube girder bridges. Proc. Int. FIB Symp. 2008 - Tailor Made Concr. Struct. *New Solut. our Soc.*, p. **178**.

[38] Z. Fu, Q. Wang, Y. Wang, B. Ji. (2018). Bending performance of lightweight aggregate concrete-filled steel tube composite beam. *KSCE J. iv. Eng.*, vol. 22, no. 10, pp. **3894–3902**.

[39] K. A. Farhan, M. A. Shallal.(2020). Experimental behaviour of concrete filled steel tube composite beams. *Arch. Civ. Eng.*, vol. 66, no. 2, pp. **235–251**.

[40] E. C. Oguejiofor, M. U. Hosain. (1997). Numerical analysis of push-out specimens with perfobond rib connectors. *Comput. Struct.*, vol. 62, no. 4, pp. **617–624**.

[41] J. H. Ahn, C. G. Lee, J. H. Won, S. H. Kim. (2010). Shear resistance of the perfobond-rib shear connector depending on concrete strength and rib arrangement. *J. Constr. Steel Res.*, vol. 66, no. 10, pp. **1295–1307**.

[42] Su, D Q. Wang. (2011). Strength and stiffness of corrugated rib connector. *Adv. Mater. Res.*, vol. 243–249, pp. **1497–1503**, doi.: www.scientific.net/AMR.243-249.1497.

[43] S. Zheng, Y. Liu, T. Yoda, W. Lin. (2016). Parametric study on shear capacity of circular-hole and long-hole perfobond shear connector. *J. Constr. Steel Res.*, vol. 117, pp. **64–80**.

[44] Li S., L. Su, Z. Sun. (2018). Research on the Load-slip Properties of Corrugated Rib Connectors' Push-out Test. *KSCE J. Civ. Eng.*, vol. 22, no. 4, pp. **1258–1264**.

[45] Ibrahim A. M., H. M. Mubarak, A. I. Said. (2018). Experimental study of push-out test of circular steel tube with various types of shear connectors. *1st Int. Sci. Conf. Eng. Sci. - 3rd Sci. Conf. Eng. Sci. ISCES* 2018 - Proc., vol. 2018-Janua, pp. **265–270**.

[46] Zheng S., C. Zhao, Y. Liu, (2018). Analytical model for load-slip relationship of perfobond shear connector based on push-out test. *Materials (Basel).*, vol. 12, no. **1**.

[47] Zheng S., Y. Y. Liu, Y. Y. Liu, C. Zhao. (2019). Experimental and numerical study on shear resistance of notched perfobond shear connector. *Materials (Basel).*, vol. 12, no. 3, pp. **1–20**.

[48] Zheng S., C. Zhao, Y. Liu, (2019). Parametric Push-Out Analysis on Perfobond Rib with Headed Stud Mixed Shear Connector. *Adv. Civ. Eng.*, vol. 2019.

[49] Chen B.C., T.L. Wang. (2009). Overview of concrete filled steel tube arch bridges in China. *Practice Periodical on Structural Design and Construction*, vol. 14, no. 2, p. **70–80**.

[50] Junghyun Cho, Jiho Moon, Hee-Jung Ko, Hak-Eun Lee. (2018). Flexural strength evaluation of concrete-filled steel tube (CFST) composite girder. *Journal of Constructional Steel Research*, vol. 151, pp. **12-24**,.

[51] Hsuan-Teh Hu, Chiung-Shiann Huang, Ming-Hsien Wu, Yih-Min Wu. (2003).Nonlinear Analysis of Axially Loaded Concrete-Filled Tube Columns with Confinement Effect. *Journal of Structural Engineering*, vol. 129, pp. **1322-1329**,.

[52] A. I. o. S. C. (AISC), Specification for Structural Steel, Chicago: AISC, 2016.

[53] Shen Z.Y., M. Lei, Y.Q. Li, Z.Y. Lin, J.G. Luo. (2003). Experimental study on seismic behavior of concrete-filled L-shaped steel tube columns. *Advances in Structural Engineering*, vol. 16, p. **1235–1247**,.

[54] Jiho Moon, Charles W. Roeder, Dawn E. Lehman, Hak-Eun Lee. (2012). Analytical modeling of bending of circular concrete-filled steel tubes. *Engineering Structures*, vol. 42, pp. **349-361**.

[55] Hosaka T., S. Nakamura, T. Umehara, K. Nishiumi. (1984). Design and experiments on a new railway bridge system using concrete filled steel pipes, Composite Construction, Conventional and Innovative, Conference Report. 1997.

[56] ASTM C494 / C494M - 17. (2019).Standard Specification for Chemical Admixtures for Concrete. https://www.astm.org/Standards/C494.

[57] ASTM 996M-05. (2019). Standard Specification For Rail-Steel and Axle-Steel Deformed Bars for Concrete Reinforcement.

[58] ACI 211.2-98 R04. (2019). Standard Practice for Selecting Proportions for Structural Lightweight Concrete.

[59] ASTM C192/C192M-05. (2019). Standard Practice for Making and Curing Concrete Test Specimens in the Laboratory.

[60] BS1881-part116:2000. (2019). Method for determination of compressive strength of concrete cube.

[61] ASTM C143 / C143M - 15a. (2019). Standard Test Method for Slump of Hydraulic Cement Concrete.

[62] ASTM C 496/C496M. (2019). Standard Test Method for Splitting Tensile Strength of Cylindrical Concrete Specimens.

[63] R. Furlong. (1967). Strength of steel-encased concrete beam-columns. *Journal of the Structural Division*, vol. 93, no. ST5, pp. **24-113**.

[64] J.-H. Ahn, C.-G. Lee, J.-H. Won, S.-H. Kim, (2010). Shear resistance of the perfobond-rib shear connector depending on concrete strength and rib arrangement. *Journal of Constructional Steel Research*, vol. 66, pp. **1295-1307**.

[65] E. Oguejiofor, M. Hosain. (1994). A Parametric Study of Perfobond Rib Shear Connectors," *Canadian Journal of Civil Engineering*", vol. 21, pp.**614-625**.

[66] U. Yoshitaka, H. Tetsuya, M. Kaoru.(2001). An experimental Study on Shear characteristics of perfobond strip and its rational strength equations. *in International Symposium on Connections between Steel and Concrete, R. Eligehausen.*

[67] B. Sara, M. Bahram. (2002).Perforbond shear connectors for Composite construction," *Engineering Journal, American Institute Of Steel Construction*", vol. 39, pp. **2-12**.

[68] C. H. Chung, J. Lee and J. S. Kim. (2015). Shear Strength of T-type Perfobond Rib Shear Connectors. *KSCE Journal of Civil Engineering*, vol. 0, no. 0, pp. **1-11**.

CURRICULUM VITAE

Yashar Hussen ALI

Education

- **M.Sc. Civil Engineering, Graduated 2022**

  University of Gaziantep College of Engineering. Civil Engineering. Dept. Gaziantep/Turkey.
- **BSc. Civil Engineering, Graduated 2001**

  AL-Anbar University /College of Engineering/ Civil Engineering Dept. /Anbar/ Iraq.
- **Secondary school education, Graduated 1991**

  AL-Ramadi High School for boys / Science Division /Anbar/Iraq.

Publication:

- 5th International Conference on Innovative Studies of Contemporary Sciences, conference papers will also be considered for publication in the special journal: "Flexural Behavior Of Concrete-Filled Steel Tube Composite Beams With Different Aspect Ratio".